Standards for dielectric elastomer transducers

Standards for dielectric elastomer transducers

Federico Carpi[1*], Iain Anderson[2], Siegfried Bauer[3], Gabriele Frediani[1], Giuseppe Gallone[4], Massimiliano Gei[5], Christian Graaf[6], Claire Jean-Mistral[7], William Kaal[8], Guggi Kofod[9], Matthias Kollosche[10], Roy Kornbluh[11], Benny Lassen[12], Marc Matysek[13], Silvain Michel[14], Stephan Nowak[15], Benjamin O'Brien[16], Qibing Pei[17], Ron Pelrine[11], Björn Rechenbach[12], Samuel Rosset[18], Herbert Shea[18]

[1] School of Engineering & Materials Science, Queen Mary University of London, London, UK
[2] The Auckland Bioengineering Institute, University of Auckland, Auckland, New Zealand
[3] Johannes Kepler University, Linz, Austria
[4] Department of Civil and Industrial Engineering, University of Pisa, Pisa, Italy
[5] School of Engineering, Cardiff University, Cardiff, UK
[6] University of Applied Sciences, Hochschule Ostwestfalen-Lippe, Lemgo, Germany
[7] University of Lyon, CNRS, INSA-Lyon, LaMCoS, Lyon, France
[8] Fraunhofer LBF, Darmstadt, Germany
[9] Inmold Biosystems A/S, Taastrup, Denmark
[10] Institute of Physics and Astronomy, University of Potsdam, Potsdam, Germany
[11] SRI International, Menlo Park, USA
[12] University of Southern Denmark, Sønderborg, Denmark
[13] Continental Corporation, Darmstadt, Germany
[14] Swiss Federal Laboratories for Materials Science and Technology, Dübendorf, Switzerland
[15] Bayer MaterialScience AG, Leverkusen, Germany
[16] StretchSense Limited, Auckland, New Zealand
[17] Department of Materials Science and Engineering, University of California, Los Angeles, USA
[18] Ecole Polytechnique Fédérale de Lausanne, Neuchatel, Switzerland

*Contact author: f.carpi@qmul.ac.uk

Smart Mater. Struct. 24 (2015) 105025 (25pp)

http://dx.doi.org/10.1088/0964-1726/24/10/105025

ACCEPTED VERSION

Abstract
Dielectric elastomer transducers consist of thin electrically insulating elastomeric membranes coated on both sides with compliant electrodes. They are a promising electromechanically active polymer technology that may be used for actuators, strain sensors, and electrical generators that harvest mechanical energy. The rapid development of this field calls for the first standards, collecting guidelines on how to assess and compare performance of materials and devices. This paper addresses this need, presenting standardized methods for material characterisation, device testing and performance measurement. These proposed standards are intended to have a general scope and broad applicability to different material types and device configurations. Nevertheless, they also intentionally exclude some aspects where knowledge and/or consensus in the literature were deemed to be insufficient. This lack is a sign of a young and vital field, whose development is expected to benefit also from this effort towards standardisation.

Keywords: Standard, dielectric elastomer, transducer, actuator, sensor, energy harvesting, electroactive polymer, electromechanically active polymer, EAP

1. Introduction

In their simplest form, dielectric elastomer transducers (DETs) consist of thin electrically insulating elastomeric membranes coated on both sides with compliant electrodes (Pelrine et al. 2000). Within the broad field of electromechanically active polymers (EAPs) (Bar-Cohen 2004, Carpi and Smela 2009), they represent a highly promising technology for actuators, strain sensors, and electrical generators that harvest mechanical energy (Pelrine et al. 2000, Carpi et al. 2008, Brochu and Pei 2010, Carpi et al. 2010, Biggs et al. 2013). The rapid development of this technology calls for the first standards that are able to provide the scientific and industrial community with guidelines on how to assess and compare performance of DET materials and devices.
This paper is aimed at addressing this critical need, presenting methods for material characterisation, device testing and performance quantification in a standardized way. This effort is the first of its kind in the DET field.
These proposed standards are intended to have a general scope and broad applicability, avoiding unnecessary prescriptions, which in some cases might be too restrictive, inadequate or inapplicable. Indeed, the huge diversity of possible DET materials (with different properties) and DET devices (with variable configurations and uses) suggest that the definition of details for many scenarios is practically impossible.
Consistently with this need for generalisation, the guidelines presented here are driven by purely physical considerations. Indeed, most parts address problems with a synthetic approach, focused more on the physical significance of procedures than on all the details of their implementation. In order to comply with specific needs, we leave to users the possibility of adapting procedures without breaking the general principles set in these guidelines.
We remark that these standards are not meant to necessarily exclude different or additional procedures that research institutes or companies may be using. Ideally, these standards should serve to reduce fragmentation in the field.
Also, we advise that this document does not constitute and should not be regarded as any sort of safety standards, as it is not meant to describe safety or safe procedures for individuals, devices or systems.
In each section below, guidelines are preceded by reminders about basic concepts, aimed at setting the context and defining the parameters and variables involved.

2. Terminology and nomenclature

Prior to presenting the guidelines, a remark about appropriate terminology is deemed to be necessary. The term ‘dielectric elastomer’ (DE) is widely accepted as the reference definition of the EAP class concerned here, i.e. a family of electrically insulating elastomeric materials (Carpi et al. 2008). Note that the term ‘elastomer’ in this context includes any long-chain polymer with significant elastic strains. The related devices should be referred to as DE transducers, which include DE actuators (DEAs), DE sensors (DESs) and DE generators (DEGs)
We discourage the use of ‘dielectric EAP’ (‘DEAP’), which is often found in the literature. The reason is that it does not identify DEs specifically. Rather, it would generally and misleadingly refer to any insulating EAP material, thus covering not only DEs, but also piezoelectric and electrostrictive polymers, as well as polymer electrets and ferroelectrets.
Standard symbols proposed for key variables and parameters are listed in table 1.

Table 1. Standard nomenclature for dielectric elastomer transducers.

Variable/parameter	Symbol	Unit
Blocking force	See	N

	'Force - electrical'	
Dielectric permittivity / dielectric constant - relative	ε_r	--
Dielectric permittivity of vacuum	ε_0	F/m
Effective actuation pressure (resultant Maxwell stress)	p	Pa
Efficiency	η	--
Electric charge	Q	C
Electric displacement	D	C/m^2
Electric field	E	V/m
Electric polarization	Pol	C/m^2
Electric potential	φ	V
Electrical capacitance	C	F
Electrical conductivity	σ	S/m= $\Omega^{-1}m^{-1}$
Electrical current	I	A
Electrical resistance	R	Ω
Electrical resistivity	$\rho=1/\sigma$	Ω m
Energy	U	J
Force - electrical (component of force exerted by the transducer when it is subject to electrical charging only)	F_e	N
Force - mechanical (component of force exerted by the transducer when it is subject to mechanical loading only)	F_m	N
Frequency	F	Hz
Frequency - angular	ω	rad/s
Imaginary unit number	j	--
Impedance - electrical	Z_e	Ω
Impedance - mechanical	Z_m	Ns/m
Loss angle - electrical	δ_e	rad
Loss angle - mechanical	δ_m	rad
Mass	m	kg
Poisson's ratio	ν	--
Power	P	W
Shear modulus	G	Pa
Strain - electrical (component of engineering strain exhibited by a transducer when it is subject to electrical charging only)	S_e	--
Strain - mechanical (component of engineering strain exhibited by a transducer when it is subject to an external mechanical loading)	S_m	--
Stress - nominal, electrical (component of nominal stress exerted by the transducer when it is subject to electrical charging only)	T_{ne}	Pa
Stress - nominal, mechanical (component of nominal stress exerted by the transducer when it is subject to mechanical loading only)	T_{nm}	Pa
Stress - true, electrical (component of true stress exerted by the transducer when it is subject to electrical charging only)	T_{te}	Pa
Stress - true, mechanical (component of true stress exerted by the transducer when it is subject to mechanical loading only)	T_{tm}	Pa
Stretch ratio - electrical	λ_e	--
Stretch ratio - mechanical	λ_m	--
Surface area	A	m^2
Surface area - active (area covered by electrodes)	A_a	m^2
Surface area - passive (area not covered by electrodes)	A_p	m^2
Temperature	$Temp$	°C
Thickness of dielectric layer	d	m
Thickness of electrode layer	d_{el}	m
Time	t	s
Time constant	τ	s
Voltage	V	V
Volume	Vol	m^3
Work	W	J
Young's modulus	Y	Pa

3. Material characterisation

3.1 Selection of the sample's thickness

For any electrical or mechanical characterisation described in the following sections, the sample's thickness might have an impact on the outcome of the measurement, as it appears from both the scientific literature (see for instance Huang et al. 2012a and Gatti et al. 2014 for the dielectric strength) and the personal experience of the authors of this paper. While the physical reasons of such behaviour are not completely understood today, at least a contribution is likely to come from the fact that obtaining samples with significantly different thickness from any given material might require different processing methods, which might use different curing conditions and might introduce different types of defects (e.g. partial cross-linking, residual solvents, etc.). These defects might be responsible, or co-responsible, for deviations that are frequently observed.

Therefore, if the characterisation is functional to a pre-defined application, we recommend that the sample's thickness is chosen to be as close as possible (according to the capabilities of the measurement setup) to the value to be used in the application.

Conversely, in the absence of application-driven specifications, for a 'general-purpose' characterisation we do not recommend here any specific thickness. Indeed, the lack of physical reasons to justify the selection of any specific value would make the choice purely arbitrary, with the risk that in some cases this choice might turn out to be inappropriate or disadvantageous, owing to the reasons described above.

3.2 Thickness of a dielectric elastomer film

3.2.1 Basic concepts

The precise measurement of the thickness of membranes used in DETs is of high importance, especially to accurately estimate an applied electric field (e.g. to work out the Maxell pressure or the breakdown strength). Due to the soft nature of elastomers used in DETs, there aren't many measurement methods that can be used. Contact methods should be avoided, as deformations can occur under the action of the probe. Methods that require knowledge of certain physical properties of the material, such as refractive index (optical methods), dielectric constant (capacitive methods), or sound speed (ultrasounds), can easily lead to significant errors, owing to the need for accurate estimates of parameters.
Optical techniques are generally preferable due to their non-contact nature. In the next sections, different optical methods are presented.

3.2.2 White light interferometry
White light interferometry (WLI) is a technique based on the short coherence length of a light beam to precisely measure the distance separating a sample from the objective, with nanometre resolution. Typically, it is used to characterize the 3D topography of a surface. To apply it to the measurement of thin membranes, it is necessary to place the sample on a flat substrate, such as a glass plate, cut a small hole (e.g. using a laser) to create a step, and measure the step height with a white light interferometer.
As an advantage, this technique has a high resolution and it gives height information over a complete surface in one fast (a few seconds) measurement, which allows for characterizing the thickness profile along different directions, to evaluate its uniformity. On the other hand, it is a destructive method due to the need for a step in the sample.

3.2.3 Laser profilometry
WLI is not the only measurement technique to determine the height of a step without any contact. A laser displacement sensor is a valid alternative, which can be used to investigate the thickness profile along directions of interest, from one edge to another, of a sample arranged onto a flat substrate.

3.2.4 Transmission or reflection spectrometry
The thickness of optically transparent thin films can be measured with transmission spectrometry, which is based on the wavelength-dependence of the transmitted intensity of a wide-spectrum beam, due to interferences created by the partial reflections at the interfaces of the film (Fig. 1).

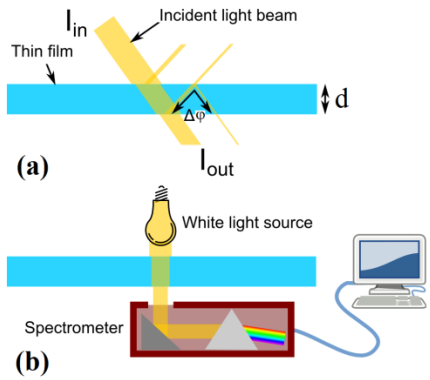

Fig. 1. (a) Transmitted light beam through a thin-film. The optical path difference (i.e. phase shift $\Delta\varphi$) between the transmitted beams modulates the output intensity as a function of the wavelength. The frequency of this modulation allows the computation of the film thickness *d*. (b) Implementation of the measurement method. A white light source sends light through a transparent thin film. The transmitted light is fed to a spectrometer, which measures the intensity as a function of the wavelength.

In case of normal beam incidence, the transmitted intensity I_{out} (which is measured with a spectrometer) shows the following dependence on the inverse of the wavelength $1/\lambda$ (Suratkar 2009):

$$I_{out} \propto 1 + a\cos\left(4\pi \cdot d \cdot n\frac{1}{\lambda}\right) = 1 + a\cos\left(2\pi \cdot f \cdot \frac{1}{\lambda}\right) \quad (1)$$

where a is a constant, d is the thickness of the membrane, and n is its refractive index. So, I_{out} versus $1/\lambda$ is a periodic signal of frequency

$$f=2nd \quad (2)$$

The value of the constant a depends on material parameters, such as the reflexion at the interfaces. However, this value is of secondary interest here, as only the frequency of the oscillations – not their amplitude – is needed to determine the thickness of the sample. Indeed, provided that the material's refractive index is known, the thickness can be obtained by simply estimating the frequency f, according to Eq. (2). To this end, it is sufficient to analyse the spectrum of the signal. Fig. 2 shows an example.

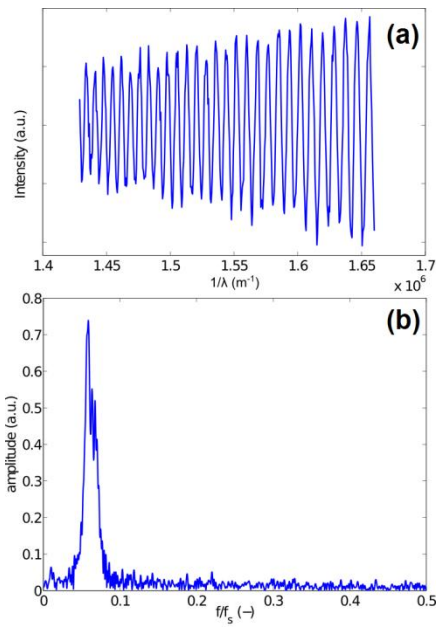

Fig. 2. (a) Transmission of a light beam through a thin PDMS: intensity is plotted as a function of $1/\lambda$. (b) A fast Fourier transform algorithm returns the spectrum of the signal (sampling frequency f_s =2mm), which shows a peak at the frequency $0.059f_s$=0.118mm. Assuming a refractive index n=1.43, this leads to a film thickness d=41.3µm.

The main advantages of this method are that it is fast and non-destructive. The main drawbacks are that it requires the film to be transparent and its refractive index to be precisely known. However, determining the refractive index using another measurement method can solve this issue. For example, WLI can be used on a set of test membranes in order to determine their thickness. Then the same membranes are characterised by transmission spectrometry, extracting the refractive index from the frequency, as their thickness is known from the WLI measurement.

As an alternative to transmission spectrometry, the thickness of a transparent membrane can also be measured with reflection spectrometry. In this case, the same approach described above can be followed, although here the membrane has to rest on a reflective substrate and the spectrometer is used to measure the reflected intensity.

3.3 Dielectric permittivity of an elastomer

3.3.1 Basic concepts

The electrical energy density stored in a DET at a given applied voltage is proportional to the elastomer's relative dielectric permittivity ε_r*, which is a complex function of the angular frequency ω:

$$\varepsilon_r^*(\omega) = \varepsilon_r'(\omega) - j\varepsilon_r''(\omega) \qquad (3)$$

The real part, also referred to as the relative dielectric constant ε_r, directly governs the amount of electrical energy available for conversion into mechanical action. As a consequence, it also determines the actual effective stress p (Maxwell's stress), i.e. the electromechanical response of the material (Pelrine et al. 2000):

$$p = \varepsilon_r \varepsilon_0 E^2 \qquad (4)$$

where ε_0 is the dielectric permittivity of vacuum and E is the applied electric field.

The imaginary part accounts for the amount of electrical energy lost as electrical dissipation in the elastomer. Hence, the full frequency spectrum of the real and imaginary parts of the permittivity completely describes the electrical storage and loss properties of the elastomer, and can help to determine whether a material may be suitable for a particular application.

3.3.2 Measurement method

Since DETs typically operate at frequencies from DC to 10 kHz, the permittivity is usually characterized within that range.

The dielectric properties should be measured by means of an instrument capable of performing a circuit impedance analysis, such as broadband dielectric analyzers, LCR bridges, potentiostats/galvanostats and vector network analysers.

The elastomer sample is sandwiched between two circular metal electrodes, forming the measurement cell schematised in Fig. 3.

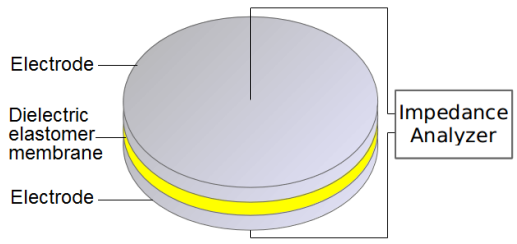

Fig. 3. Schematic drawing (not in scale) of a typical setup to measure the dielectric permittivity of an elastomer.

The cell is a parallel plate capacitor, whose complex capacitance C* is proportional to ε_r* of the elastomer:

$$C^*(\omega) = \varepsilon_0 \cdot \frac{\varepsilon^*(\omega)A}{d} \qquad (5)$$

where A is the area of the electrodes and d is the thickness of the elastomer film. The circular geometry is recommended, so as to avoid inhomogeneity in the electric field distribution.

A sinusoidal current is applied to the cell, and the voltage response is analysed in terms of amplitude and phase shift with respect to the current. Real and imaginary parts of the relative permittivity at any given frequency can be obtained by means of a circuit analysis. The frequency is then changed and the measurement procedure repeated, until the desired frequency range is covered.

To identify possible contributions from both electrodes' polarisation and electrophoretic conductivity from impurities (which is fundamental to assess the material bulk properties), it is recommended that both the real and imaginary parts of the permittivity spectra are presented. The imaginary part can even be displayed as the so-called loss tangent:

$$\tan\delta = \frac{\varepsilon_r''(\omega)}{\varepsilon_r'(\omega)} \quad (6)$$

It is recommended to keep the wires connecting the cell to the measurement instrument as short as possible, so as to minimize the circuit's electrical spurious components (wiring impedances, contact resistances, parasitic impedances). In particular, this is of great importance for two-points measurements (as opposed to four-points measurements), in which case a determination of the parameters of the circuit's portion external to the sample cell must be preliminary accomplished by a proper calibration. Such a calibration can be carried out by measuring the response spectrum of the cell hosting a reference, loss-free, dielectric material, such as poly-tetrafluoroethylene (PTFE or Teflon^{TM}). Choosing reference specimens with sizes close to those of the samples that are going to be tested will result in a more accurate calibration.

If the frequency is increased over 100MHz, wavelengths become so short that the system starts to behave more like a distributed parameters network, rather than a concentrated constant circuit, so that more complex setups and procedures are required.

Besides a dependence on temperature and humidity (as for any polymers), the dielectric properties of elastomers can be affected by the applied pre-stretch (Kofod at al. 2003, Choi et al. 2005, Wissler and Mazza 2007, Troels et al. 2013), revealing that the electromechanical response might have an electrostrictive component. Hence, data should always be accompanied by information on the measurement conditions.

3.3.3 Sample preparation

The sample should be prepared from a thin film of elastomer. The ratio between the electrode area and the film thickness should be as high as possible, preferably such that $\sqrt{A}/d \geq 100$, so as to minimize field fringe effects.

The selection of the thickness should be done according to the considerations reported in section 3.1. Moreover, the actual value of the thickness needs to be measured carefully, using the methods recommended in section 3.2.

Accurate control of both the area A and thickness d is necessary. While the measurement of A is typically easy, the measurement of d is challenged by the material softness, such that the use of optical techniques is recommended (see section 3.2).

Proper contact between the cell's electrodes and the elastomer should be ensured, so as to limit interfacial polarisation of the elastomer at the electrodes. To this end, the elastomer surface should be metallised (by means of metal evaporation or sputtering) or coated with conductive media, such as powdered metals (e.g. gold).

The use of conductive pastes or greases (such as carbon grease) as media to interface the cell's electrodes and the elastomer is discouraged, due to possible penetration of the liquid fraction of the electrode medium into the elastomer. Further, such media have low conductivity (as compared to metals) and therefore introduce significant additional electrical impedance in series, which gives rise to problems with repeatability between measurements.

The use of compliant conductive materials as cell electrodes should be avoided if the measurement is performed at electric fields sufficient to induce significant deformations.

3.3.4 Dielectric permittivity at high electric fields

It is worth stressing that the DET scientific literature presents (nearly exclusively) permittivity data obtained with measurements at electric fields at least one-order-of-magnitude lower than those typically used for actuation. This is due to the type of instrumentation most commonly available in laboratories. More accurate investigations would require that the dielectric properties are measured at the electric fields actually used in the application of interest. This need calls for equipment for high-voltage dielectric spectroscopy.

In the lack of such equipment, the effective dielectric constant at high electric fields can be estimated by fitting data obtained from a pure-shear isometric test, as described later in section 3.7.4.

3.4 Dielectric strength of an elastomer

3.4.1 Basic concepts

The electromechanical performance of a DET is ultimately limited by the electrical breakdown strength of its constitutive elastomer, also called dielectric strength. Electrical failure is characterized by a sharp increase of current, occurring when a critical voltage threshold is reached. With reference to a planar DET, the dielectric strength E_{crit} is defined as the ratio between the critical breakdown voltage V_{crit} and the film thickness d:

$$E_{crit} = \frac{V_{crit}}{d} \quad (7)$$

Dielectric strength values of typical DET materials are of the order of 10 or 100 V/µm. The consequence of electrical failure is usually permanent, as a conductive path is created through

the elastomer, preventing the device to be charged again.

In addition to a dependence on extrinsic factors, such as humidity, temperature, the type (constant or variable), rate and duration of the electrical stimulation, as well as the stiffness, geometry, size and surface properties of the electrodes (and the force that they apply), the dielectric strength typically varies also with the material elastic modulus (Kollosche and Kofod 2010), the sample thickness (Huang et al. 2012a, Gatti et al. 2014) and the applied pre-stretch (Kofod at al. 2003, Choi et al. 2005, Huang et al. 2012a, Troels et al. 2013, Gatti et al. 2014). Moreover, the dielectric strength relates to the threshold value of current that has been set to define a breakdown event.

Hence, data should always be accompanied by detailed information on the above-mentioned properties of the elastomer sample, properties of the electrodes, conditions of measurement and adopted threshold for the current.

3.4.2 Measurement method

So far, a widely shared consensus on how to measure the dielectric strength of soft elastomers is not available, especially with reference to uses for DETs.

An apparatus that can be adopted to that effect is sketched in Fig. 4 (Kollosche and Kofod 2010).

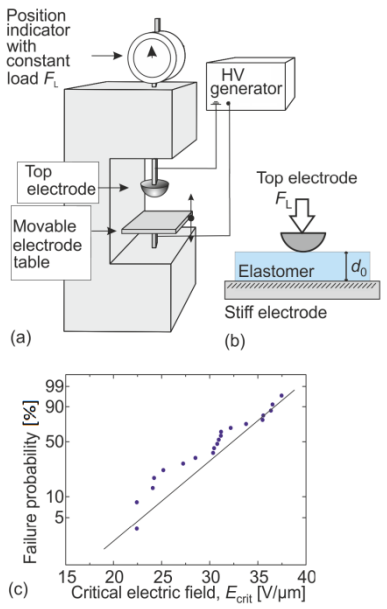

Fig. 4. (a) Schematic drawing of an apparatus to measure the breakdown strength of elastomers. (b) Hemispherical top electrode which rests with known force F_L on the elastomer film of initial thickness d_0. (c) Example of data analysis using a Weibull plot.

The film should have an area of at least 1 cm^2 and a uniform initial thickness d_0.

The selection of the thickness should be done according to the considerations reported in section 3.1. Moreover, the actual value of the thickness needs to be measured carefully, using the methods recommended in section 3.2.

The film is placed on a flat polished metal slab functioning as the ground electrode. The active electrode is a rounded piece of metal, which should be polished and free from irregularities resulting from previous testing (ASTM D149-09(2013) standards).

The active electrode rests on top of the sample, with a constant force F_L, so as to ensure contact. The applied force causes the thickness of the film to change by a certain amount. It is recommended to limit this initial compression, as much as possible, and in any case to take it into account when data are processed. From this initial condition, the voltage is increased as a ramp until electrical breakdown occurs, as detected by a sudden raise of current, which usually causes the voltage to drop down (according to the maximum power that can be delivered by the voltage source). The ramp slope should be reported.

We remark that the so-measured dielectric strength of an elastomer can never be regarded as representative of the electrical breakdown properties of any transducer made of that material, owing to effects introduced by the electrodes and boundary constraints.

3.4.3 Statistical analyses

Electrical failure is a statistic event and must be evaluated using a statistical approach. The use of the Weibull distribution (Weibull 1951) is recommended. As an example, we refer to (Kollosche and Kofod 2010).

3.4.4 Complementary mechanical testing

The dielectric strength is typically correlated to the mechanical stiffness of the elastomer (Kollosche and Kofod 2010). So, if testing is aimed at characterising a 'general-purpose' material, for comparison purposes it can be useful to accompany the dielectric characterisation with a mechanical one.

3.5 Quasi-static mechanical characterisation of an elastomer

3.5.1 Basic concepts

An elastomer typically deforms at large strains with a nonlinear behaviour that depends on elastic and inelastic phenomena. The former is best captured by a hyperelastic description, for which a strain energy function exists (Ogden, 1997), while the latter comprise viscosity and stress softening mechanisms, such as the Mullins effect (Mullins 1969).

Typical tests used to characterise mechanical properties of elastomers are the uniaxial tensile or compressive test, the pure shear test and the biaxial test.

For uniaxial, compressive and pure shear tests, different definitions of stress and strain (nominal or true) can be employed to process and present data. Stress-strain data are better reported in terms of nominal (engineering) strain

$$S_m = \frac{(L-L_0)}{L_0} = \lambda_m - 1 \quad (8)$$

where L is the current length of the stretchable part that initially corresponds to L_0 and $\lambda_m = L/L_0$ is the longitudinal stretch, and nominal stress

$$T_{nm} = \frac{F_m}{A_0} \quad (9)$$

where A_0 is the initial cross-section of the specimen, and F_m is the applied force.

When the evaluation of the actual stress and strain is necessary, true strain S_{tm} and true stress T_{tm} are calculated taking into account the specimen's current cross section A ($A = A_0/\lambda_m$ due to incompressibility), respectively as follows:

$$S_{tm} = \ln \lambda_m \quad (10)$$

$$T_{tm} = \frac{F_m}{A} \quad (11)$$

Following the mechanical tests, the stress-strain curve should be presented and the following information should be specified:

i) At least the Young's modulus (or elastic modulus) Y, that is the constant of proportionality between stress and longitudinal strain in the small-strain regime (i.e. the tangent modulus at 0% strain), for a uniaxial test performed from the natural configuration (sample at mechanical rest without deformations). Note that, as incompressibility is a common assumption for elastomers (the volume is maintained constant upon deformation), we have $Y=3G$, where G is the shear modulus in the natural configuration (initial shear modulus). Also, note that for a pure shear test the tangent modulus at 0% strain corresponds to (4/3) Y. Furthermore, a plot of the tangent modulus over the whole range of strain explored might be of interest.

ii) The position of the inflection (flex) point in the nominal stress-strain curve (if not evident from the plot);

iii) The stress and strain at break (if not evident from the plot);

Fig. 5 visualises these quantities with reference to a uniaxial tensile test.

For a biaxial test, the methodology to infer the true stress from the value of the in-plane stretch is described in section 3.5.2.

As previously recalled, the simple framework to build a model able to describe the nonlinear behaviour of elastomers is hyperelasticity (Ogden, 1997). Many different hyperelastic strain energies exist, such as Mooney-Rivlin, Ogden, Arruda-Boyce, Gent, the latter being often used to model DEs because of its ability to predict a finite maximal stretch of the material with a few parameters (for a concise overview of the main hyperelastic models see Carpi and Gei, 2013). However, before choosing any particular strain energy, it is necessary to apply it to experimental stress-stretch data to evaluate its actual ability to accurately describe the mechanical behaviour of the elastomer being tested.

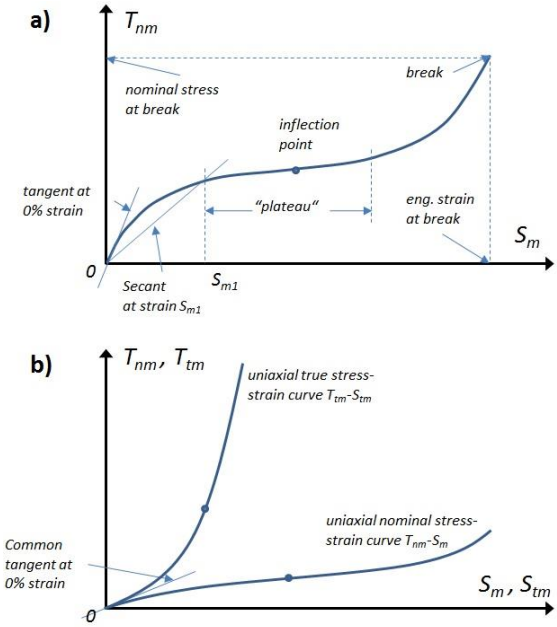

Fig. 5. a) Sketch of a typical uniaxial tensile nominal stress T_{nm} versus nominal strain S_m curve of a cross-linked elastomer. The Young's modulus Y corresponds to the tangent at 0% strain. b) Comparison between uniaxial nominal stress T_{nm} and true stress T_{tm} versus strain curves; the inclination of the tangent at the origin coincides for the two plots.

When large deformations are considered and a hyperelastic model is fitted to experimental data, plots should preferably be presented using the true stress as a function of the stretch ratio, so as to facilitate the use of hyperelastic models.

Elastomers are subject to the Mullins effect, a stretch-induced softening of the material, as shown in Fig. 6 (Mullins 1969).

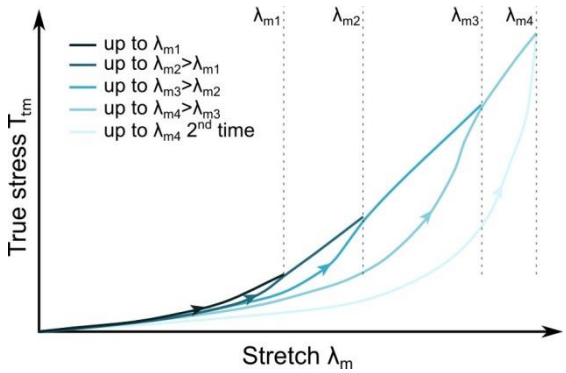

Fig. 6. Illustration of the Mullins effect: an elastomer sample is stretched to increasingly larger maximal stretch ratios (λ_{m1} to λ_{m4}). Once the maximal stretch is reached, the sample is relaxed to a stretch of 1 (relaxation not shown on the graph). The Mullins effect causes a softening of the material depending on the maximal

stretch that the sample has experienced previously. When the sample reaches a stretch zone it has not yet experienced, its stress-stretch characteristic presents an abrupt change of slope.

Owing to the Mullins effect, the mechanical properties of an elastomer (Young's modulus, or parameters of a hyperelastic model) depend on the maximal stretch that the sample has been submitted to, during its life.
It is worth noting that it is necessary to subject the sample to more than one loading-unloading cycle, as the stretch-induced softening occurs mainly between the first and second cycle (Mullins 1969), as shown in Fig. 7.

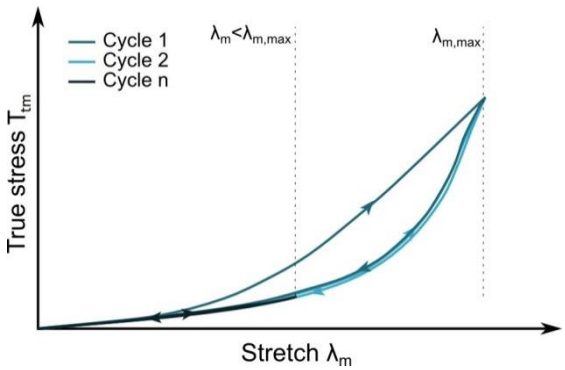

Fig. 7. Cyclic stretching of an elastomer up to a given maximal stretch $\lambda_{m,max}$ shows that the Mullins effect occurs mainly between the first and second cycle. Further cycling will return a curve similar to that of cycle 2. If one of the cycles (cycle n) goes to a maximal stretch value smaller than $\lambda_{m,max}$, then it will still follow the behavior of cycle 2. Only if $\lambda_{m,max}$ is exceeded, the curve will change, as shown in Fig. 6. The cycles shown here are obtained with a sufficiently small deformation rate to neglect viscous losses in the material, i.e. there is no loss-induced hysteresis. A Mullins-induced hysteresis occurs mainly in cycle 1, as represented in the graph.

The Mullins effect can be modelled within a pseudo-elasticity approach, as shown by (Ogden and Roxburgh 1999).

3.5.2 Measurement method

The recommended measurement apparatus for uniaxial tests is represented by standard uniaxial testing machines.
For pure shear tests, the same machines can be used, although with a different grip system (Rivlin and Saunders 1951).
Equi-biaxial testing can be performed using a bubble inflation technique: a circular membrane is clamped on a circular frame and inflated with a known pressure. The stretch at the apex of the bubble is measured with optical means, and the equi-biaxial stress-stretch curve can be calculated from the geometry of the membrane, the applied pressure, and the stretch of the bubble (Reuge et al. 2001):

$$T_{tm} = \frac{P R_c \lambda_m^2}{2 d_0} \qquad (12)$$

where T_{tm} is the equi-biaxial true stress, P is the applied pressure, λ_m is the membrane stretch, R_c is the radius of curvature of the bubble and d_0 is the initial thickness. It is important that both λ_m and R_c are measured at the centre of the membrane, as only that point is in a state of purely equi-biaxial stress. This is often done by delimiting a zone of interest on the membrane.
It is worth stressing here the following important consideration. While DE membranes are often prestretched and activated equi-biaxially, their mechanical characterisation is frequently performed using a uniaxial pull test, because it is easier to perform. However, it is worth noting that inferring the equi-biaxial behaviour of a material based on a uniaxial pull test could be not accurate (see Boyce and Arruda 2000 and Rosset et al. 2014). So, we recommend that any material of interest is characterised, when possible, with uniaxial, pure shear and equi-biaxial mechanical tests and the combined tests are used to fit a material model.
Any kind of test should be performed at a constant deformation rate. Readings are taken during uninterrupted stretching of the test piece.
The selection of the deformation rate is critical. Indeed, stress-strain curves vary as a function of the deformation rate. Owing to a significant variability among DE materials in terms of elongation at break and viscosity, no specific value of deformation rate is recommended here, so as to avoid excessive prescriptions. Indeed, guidelines reported by some standards on materials characterisation (such as a deformation rate of 1% of the initial length per minute, as recommended by EN ISO 527-1, 1996-04) might be too restrictive for some elastomers that are highly stretchable and are meant to be characterised up to several hundred percent strain.
While we do not prescribe any specific deformation rate, we recommend the following procedure. First, the characterisation is repeated using two different deformation rates $\dot{\lambda}_1$ and $\dot{\lambda}_2$, with $\dot{\lambda}_2 = 10\dot{\lambda}_1$. If results will show a deviation higher than 10%, then the test should be repeated with a third deformation rate $\dot{\lambda}_3 = 0.1\dot{\lambda}_1$. If $\dot{\lambda}_3$ results differ from those of $\dot{\lambda}_1$ by more than 10%, then the iterative process should continue by scaling down the deformation rate until no significant changes will be observed.
Once the deformation rate has been selected, each mechanical test should be repeated two or three times, up to the same stretch, in order to take into account the possible stretch-induced softening (Mullins effect), as shown in Fig. 7. The stretch range should be selected in accordance with the envisaged application (taking into account both the pre-stretch and the expected actuation stretch), as the mechanical behaviour of any elastomer depends

on the stretch range it has been submitted to during its life (Rosset et al. 2014).
The mechanical properties of elastomers are sensitive to environmental conditions, especially temperature and humidity (see, for instance, Oertel 1993). Thus, for comparison purposes it is recommended to adopt, if possible, the following standard conditions: 23±2 °C and 50±5% rh.

3.5.3 Sample preparation and conditioning
The recommended sample's shape depends on the test. For uniaxial tensile tests, the dumb-bell (or dog bone) shape is preferable, according to standard practice for tensile testing in general (see for instance Type 2 specimen in ISO 37, 5th ed. 2011-12-15).
For pure shear tests, the specimen should be much shorter in the stretching than in the width direction: a ratio of height to width of at least 1:5 (preferably 1:10) is recommended (Treloar 1944, Kollosche et al. 2012).
For biaxial tests, a circular membrane with thickness much smaller than its diameter should be used, so that the bending energy can be neglected. The zone of interest at the centre of the membrane on which the radius of curvature and stretch are measured should be at least 5 times smaller than the membrane diameter. Furthermore, the technique used to visually delimit this zone must not alter the mechanical properties of the material under test. Carbon black or other types of powders are suggested as a suitable choice, as they are not expected to introduce any significant stiffening of the membrane. Differently, the use of pastes or greases is discouraged as they might release a liquid fraction, which might change the mechanical properties of the elastomer membrane more or less significantly, according to several factors (such as amount of material, diffusion coefficient and duration of the test).
For material cutting, fixed blades are preferable to moving knife techniques, so as to improve accuracy (see for instance the cutters described in ISO 23529:2012-10).
The selection of the thickness should be done according to the considerations reported in the dedicated section 3.1. Moreover, the actual value of the thickness needs to be measured carefully, using the methods recommended in section 3.2.
Specimens need to be conditioned before testing. Prescriptions described in ISO 23529:2012-10 are recommended, implying a conditioning time of at least 16 hours before the measurement, where the time to temperature equilibration is significantly shorter (a few minutes for films with a thickness of the order of 100 µm or less) than the time to humidity equilibration, which depends on the material hydrophilicity (Danfoss 2014, Moreno et al. 2012).

3.6 Surface (or sheet) resistance of compliant electrodes

3.6.1 Basic concepts
Besides compliance, a key property of DET electrodes is their electrical resistance, which depends on the volume (or bulk) resistivity of the constitutive material and the amount of material deposited. As the electrode thickness depends on the fabrication process and is not easy to measure, it is not effortless (sometimes not even possible) to compare the resistivity of different electrode materials by simply measuring the electrode resistance. This problem can be faced by measuring the surface (or sheet) resistance, which best quantifies the electrical properties of a thin electrode layer, along the surface plane (not perpendicularly to it, i.e. not along the thickness direction).
For an electrode of thickness d_{el}, length L and width w, made of a homogenous material of volume resistivity ρ, the volume (or bulk) electrical resistance R along the length is given by

$$R = \rho \frac{L}{w\, d_{el}} \tag{13}$$

The surface (or sheet) electrical resistance R_s of the electrode is defined as

$$R_s = R\frac{w}{L} = \frac{\rho}{d_{el}} \tag{14}$$

Thus, the physical units of a surface resistance are Ω. However, its conventional units are "Ohm per square" and are denoted as Ω/sq or Ω/□, which are dimensionally equivalent to Ω but allow for univocally distinguishing a surface resistance from a volume resistance. These units are justified by the fact that the surface resistance of a square surface (L=w) coincides with its volume resistance and is independent of the square's size. So, the surface resistance can be defined as the volume resistance of a square electrode of any size, and its units "Ohm per square" can be regarded as a sort of "Ohm per aspect ratio".

3.6.2 Measurement method
The following method is recommended to measure the surface resistance of thin layers of conductive material, so as to evaluate various electrode materials (e.g. dry powders, greases, inks, etc.) and fabrication techniques (e.g. smearing, printing, plotting, spraying, etc.).
A long and thin rectangular strip of homogeneous conductive material is prepared on an insulating substrate. The suggested length L_s ranges from 5 to 50 mm. The thickness of the conductive layer can be unknown.
To avoid the measurement of contact resistances, the following four-point probes method is adopted. The strip is contacted at each end by a bar electrode covering the whole width of the strip. A constant current I is injected in the sample via the two bars.

Two probes are then used to measure with a high-impedance voltmeter the voltage drop V between any two points separated by a distance L in between the current-injecting bars. The setup is schematised in Fig. 8. We advise that the two probes are applied without exerting any significant pressure to the strip, so as to avoid significant deformations, which might alter the reading.

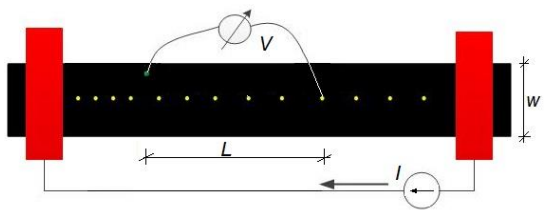

Fig. 8. Setup for the measurement of the surface resistance of a thin layer of a conductive material.

A high aspect ratio L/w in the order of 10:1 (at least 5:1) ensures a homogeneous current flow, at least in the central portion of the sample.
The surface resistance of the portion of the sample delimited by the length L can thus be calculated as follows:

$$R_s = R\frac{w}{L} = \frac{V}{I}\frac{w}{L} \quad (15)$$

In order to assess the quality of the electrode in terms of uniformity, the following finer investigation can also be performed. A probe is used to measure the electrical potential φ at various positions (between the current-injecting bars) with respect to any arbitrary reference point. For an electrode shaped as a long rectangular strip with uniform distribution of its constitutive material in any direction, φ will be a function of only the axial coordinate x along the length direction (at least in the central portion of the sample) and this function will be linear.

3.6.3 Measurements under stretching

One of the key properties of electrodes for DETs is the ability to remain conductive under stretching. It is therefore important to characterize the resistance not only in the non-deformed state, but also when the electrode is stretched (possibly over multiple cycles).
To this aim, the method described above should be used in combination with a stretching apparatus. However, we discourage the use of uniaxial extension. Indeed, in such a condition the electrode's conductive elements gets closer to each other in the planar direction perpendicular to stretching, thus leading to a measurement which is not representative of an actual expansion of the whole electrode. Therefore, we recommend the use of a bi-axial extension test.

3.6.4 Complementary mechanical testing

Compliant electrodes for DETs should not only remain conductive when stretched, but also have little impact on the stiffness of the overall transducer. So, if testing is aimed at characterising a 'general-purpose' electrode material, for comparison purposes it can be useful to accompany the electrical characterisation with a mechanical one.

3.7 Electromechanical transduction performance of an elastomer with compliant electrodes and applied pre-strain

3.7.1 Basic concepts

The following sections present guidelines to characterise the transduction properties of materials for DEAs, according to the most used tests: pure shear (with uniaxial pre-strain) and expanding circle (with bi-axial pre-strain).
Nevertheless, it is worth stressing that these two configurations do not necessarily lead to the maximisation of the achievable strain. Indeed, the adopted configuration and the application of unequal pre-stretches in different directions can lead to a complex interplay of nonlinear processes (Kollosche et al. 2012). In particular, it has been shown that, by applying a uniaxial pre-strain and measuring the electrical strain in transverse direction, the output can be higher as compared to both a pure-shear and a biaxial-pre-strain test (Akbari et al. 2013).

3.7.2 Compliant electrode material

The electromechanical transduction performance of any elastomer with compliant electrodes is typically dependent on the electrode material (Rosset and Shea 2013, Carpi et al. 2003). Therefore, if the destination of use of the elastomer is already defined, the test should be performed with the same electrode material envisaged for the final application, which is likely to be dictated by specific requirements and constraints.
If the electrode material is not imposed by any specifications, samples should be prepared such that the limitation of the electrical strain due to the electrodes' stiffness is minimized. To this end, conductive greases or particles are recommended. If a choice is possible, carbon grease is of preference, because of a typically high conductivity, an ability to form surfaces with uniform distribution of charge, as well as ease of use. Thin layers of conductive elastomer composites might be adopted as well, although their actual impact in terms of stiffening should be assessed with comparative stress-strain measurements.

3.7.3 Electrical contacts

An electrical contact is defined as the interface between a compliant electrode material and an electrical lead. If the type of contact is not prescribed by any specifications, metals (e.g.

aluminium or copper) are recommended as suitable materials, which can be used in a diversity of possible forms (as more practical for the test), such as free-standing stripes or various shapes etched on the surface of printed circuit boards (also used as mechanical supports). As the electrical contact edges typically concentrate electrical charges, which raise the electric field locally, care should be exerted to ensure that the contact region is not superimposed to the counter-electrode on the other side of the elastomer layer, in order to prevent premature electrical breakdown.

3.7.4 Uniaxial actuation mode: pure-shear configuration

The pure-shear configuration is aimed at making any spatial variation of strain and electric field negligible over the sample (Kofod and Sommer-Larsen 2005). This uniformity makes the test largely independent of the boundary conditions introduced by the frames that support the elastomer. To this end, the specimen has to be flat and much shorter in the stretching (length) than in the other (width) direction, as represented in Fig. 9. A length-to-width ratio of at least 1:5 (preferably 1:10) is recommended (Kollosche et al. 2012). This configuration also allows for a large active-to-passive area ratio, limiting the mechanical resistance offered by the passive (uncoated) area of the elastomer film.

The static electromechanical performance should be assessed with two measurements (Fig. 9): i) isometric (or isostatic) test, where the strain is maintained constant and the force is measured upon electrical driving; ii) isotonic test, where the force is maintained constant and the strain is measured upon electrical driving.

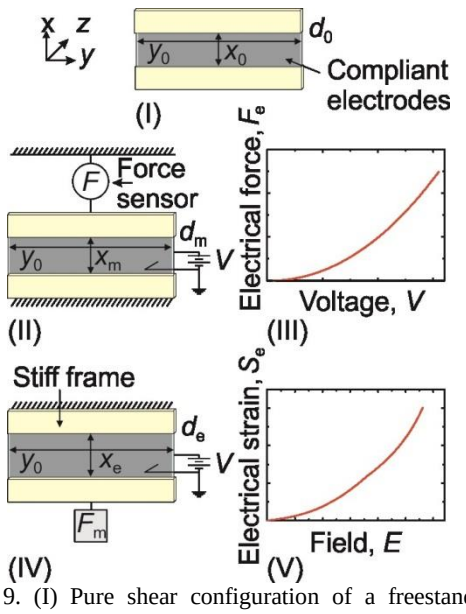

Fig. 9. (I) Pure shear configuration of a freestanding elastomeric membrane with length x_0 width y_0 and thickness d_0. (II) Isometric test: the sample is mechanically stretched to a length x_m resulting in a thickness d_m and a mechanical force F_m, which then decreases by an amount F_e representing the electrical force generated by applying a voltage V. (III) Isometric test: typical voltage - electrical force curve. (IV) Isotonic test: while the sample is subject to a constant mechanical force F_m, an applied voltage V causes a length x_e and thickness d_e. (V) Isotonic test: typical field – electrical strain curve.

The isometric and isotonic experiments not only return a characterization in terms of electrical strain and stress, but also allow for estimates of relevant material parameters. In particular, the effective dielectric constant ε_r can be obtained by fitting the isometric data with the following function

$$F_e = \frac{\varepsilon_0 \varepsilon_r y_0 V^2}{d_m} \quad (16)$$

which correlates ε_r to the measurable force F_e and applied voltage V.

The measurement of the electrical strain S_e

$$S_e = \frac{x_e - x_m}{x_m} \quad (17)$$

and the condition of volume conservation

$$d_0 x_0 y_0 = d_e x_e y_0 = d_m x_m y_0 \Rightarrow$$
$$d_0 x_0 = d_e x_e = d_m x_m \quad (18)$$

allow for a calculation of the true electric field E_t:

$$E_t = \frac{V}{d_e} = \frac{V\, x_e}{d_m x_m} \quad (19)$$

Fitting the isotonic data with the function

$$S_e = \gamma E_t^2 \quad (20)$$

returns the electro-mechanical sensitivity γ, which depends on the elastomer's dielectric constant and stiffness at the working strain.

So, these equations enable simple analyses, under the assumption that stress, strain and applied electric fields are uniform throughout the specimen. Samples for pure shear testing are prepared by fixing to the elastomer film rigid clamps, which define a freestanding membrane of desired length-to-width ratio. The freestanding area is coated with complaint electrode material.

The recommended measurement apparatus is a double- (or single-) column dynamometer for uniaxial mechanical testing, capable of position and force control.

3.7.5 Biaxial actuation mode: expanding-circle configuration

The electrically induced biaxial deformation of the active area of a circular DEA consisting of a membrane pre-stretched on a circular frame is a useful test to evaluate new elastomers, electrodes and their combinations (Pelrine et al 2000).

It is worth noting that an expanding circle test could also be performed by pre-stretching the elastomer with a dead load, which would allow for much higher strains (Huang et al 2012b). Nevertheless, as compared to a pre-stretch by dead load, we recommend a pre-stretch by rigid frame, as it is easier to implement.

Let's refer to a cylindrical coordinate system r, θ, z, with z aligned along the thickness direction. When

the circular electrodes are electrically charged, the elastomer's thickness decreases from a value d_0 at rest to a value d_e, while the active radius and area respectively increase from R_0 and A_0 to R_e and A_e, as sketched in Fig. 10.

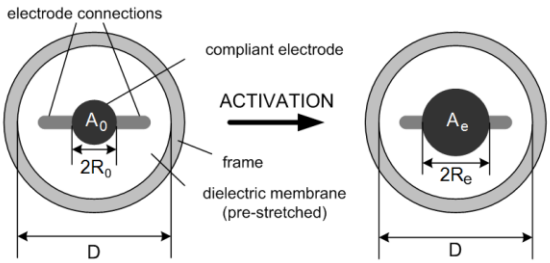

Fig. 10. Circular DEA in the non-activated state (left) and in an electrically activated state (right).

By considering the stretch ratio λ_z along the axial direction

$$\lambda_z = \frac{d_e}{d_0} \tag{21}$$

and by taking into account that the elastomer's incompressibility leads to

$$d_e A_e = d_0 A_0 \tag{22}$$

we have

$$\lambda_z = \frac{d_e}{d_0} = \frac{A_0}{A_e} = \frac{R_0^2}{R_e^2} = \frac{1}{\lambda_r^2} \tag{23}$$

where λ_r is the stretch ratio along the radial direction. So, the variation of the thickness can be obtained by measuring the change of the electrodes' radius or area.

It is worth noting that Eq. (23) can also be obtained by combing the incompressibility condition

$$\lambda_r \lambda_\theta \lambda_z = 1 \tag{24}$$

with the following relation, due to homogeneity of the deformation in the active area:

$$\lambda_\theta = \lambda_r \tag{25}$$

Eq. (23) can also be re-written in terms of thickness strain $S_{e,z}$ and radial strain $S_{e,r}$ as follows:

$$S_{e,z} = \frac{1}{\left(S_{e,r}+1\right)^2} - 1 \tag{26}$$

To perform this test, an elastomer membrane (usually a single layer) has to be pre-stretched equi-biaxially in a controlled manner (possibly using a radial stretching apparatus). Then, while the membrane is pre-stretched, it is mounted on a rigid frame having a circular hole. The hole should have a diameter at least three, possibly ten (Koh, Li et al. 2011), times larger than that of the desired electrode. Such a ratio is aimed at making the reduction of the tensile elastic force exerted by the passive (electrode-free) annular region on the central active region negligible, while the latter electrically expands. This makes pre-stretching close to that provided by a dead load (i.e. constant force), which is known to enable the maximum electrical strain (Huang et al 2012b).

Finally, circular electrodes are created in the centre of the membrane and compliant conductive paths are realized to connect each electrode to the boundary of the frame, where the electrical connections are made (Fig. 10).

To measure the electrically induced radial or area strain, we recommend the use of a contact-less optical technique, such as processing of images acquired with a digital camera. However, care should be paid to the fact that the actual extension of the active area may not correctly be captured by optical techniques, if large out-of-plane deformations (such as wrinkles due to loss of tension) occur. To overcome this problem, the recommendation is to use a pre-stretch sufficiently high to avoid loss of tension, provided that the amount of pre-stretch is not pre-defined.

Alternatively, indirect measurements of the electrically induced strain could be obtained with electrical tests, recording the capacitance with an LCR meter (Keplinger et al. 2008). However, capacitive measurements might not necessarily offer the highest possible accuracy, as they are affected by a different problem: depending on the elastomer material, the dielectric permittivity might vary more or less significantly according to the strain (Kofod at al. 2003, Choi et al. 2005, Huang et al. 2012a, Troels et al. 2013, Gatti et al. 2014) and the electric field, although the latter effect is poorly studied at present (Rosset at al. 2013). An unknown variation of the permittivity might result in a wrong estimate of strain from a reading of capacitance. To overcome this problem, the recommendation is to characterise in advance the dependence of the material permittivity on the strain and the electric field, according to the procedures described in section 3.3.

3.7.6 Pre-strains (2.6.2.5)

Any elastomer exhibits different actuation performance depending on the applied pre-strain, because of a shifting or suppression of electromechanical instability (Koh et al. 2011). So, the choice of the pre-strain is important when performance is characterised. We describe below two methods of pre-strain selection: one method (preferable) is based on optimal values, the other is not.

The optimal pre-strain selection method is aimed at maximising the electrical strain, either the one achievable at "low" electric fields or the one at "high" fields. The former strain is obtained with a pre-strain that minimises the slope of the (uniaxial or biaxial) engineering stress-strain curve, i.e. the point of maximum compliance (see for instance (Carpi and De Rossi 2005)). The latter strain (which is also the highest achievable strain, in absolute terms) is obtained with a pre-strain (usually higher than in the previous case) that suppresses electromechanical instability (Suo 2010,

Koh et al. 2011), allowing the elastomer to be driven at higher fields. Once the optimal pre-strain of interest has been selected (in the first case experimentally, in the second case theoretically), tests can be carried out with different pre-strains around this value, so as to verify the maximisation of the electrical strain.
The non-optimal pre-strain selection method uses a pre-defined set of pre-strain values. We suggest the following progression set: 10%, 30%, 50%, 100%, 150%, 200%, etc. (according to the material's capabilities).

3.7.7 Sample preparation and conditioning
The selection of the elastomer's thickness should be done according to the considerations reported in section 3.1. Moreover, the actual value of the thickness needs to be measured carefully, using the methods recommended in section 3.2.
Any electrode material should be applied shortly before the beginning of the test, so as to minimise the effect of a possible penetration (diffusion) within the elastomer, especially when the material is able to release a fluid phase.
The measurement of electrically induced strains/stresses should start when the sample has reached a steady state after creep/stress relaxation, ideally. In practice, measurements are recommended only when the length/force variation over time is lower than 5% at least.

3.7.8 Electrical driving
The characterisation should be done by applying voltage ramps or step-wise voltages of different amplitude, until electrical failure occurs.
In order to characterise quasi-static behaviour, voltage ramps are preferable to step-wise voltages, as they allow for investigations of the electrical response with continuity, up to electrical breakdown. To this end, the ramp's slope should ideally be as low as possible. Nevertheless, excessively small slopes might make test unpractically long, which suggests the need for trade-off values. As the literature doesn't offer today evidences that justify the prescription of a maximum slope, i.e. a minimum time to breakdown, here we arbitrarily recommend (as an operative guideline) that the latter should be at least 3 minutes.
Step-wise voltages also allow for characterizations also of the transient response, in addition to the steady-state static response. In this case, attention should be paid to the fact that the charging speed might be limited by the slew rate and/or the maximum output current of the electrical source. It is therefore necessary to ensure that the charging time is shorter than the mechanical response time of the elastomer.

3.7.9 Presentation of data
When reporting results, a stretch ratio should be preferable to strain, for at least two reasons: it avoids any risk of confusion between engineering and true strain, and it matches common practice in hyperelastic energy density models, which always use stretch ratios. Nevertheless, the use of stretch rather than strain is not meant here to represent any prescription, as we recognise that many users are more used to the latter and might still prefer it. The only recommendation is that, in case of use of strains, clear indications are reported as to whether values refer to the engineering or true strain definition.
Moreover, intensive measures like stretch ratio (or strain), stress and electric field (or voltage per unit thickness) are in general preferable to extensive measures like deformation (variation of a given dimension), force and voltage, respectively. This is justified by the fact that normalised variables make the description of performance independent of the size of the sample or amount of material. Nevertheless, it is recognised that explicit information about deformations, forces, and voltages can be practically useful in some cases. So, if this information is given, we advise that it represents an addition and not an alternative to the normalised values.
Also, it should be clearly specified whether the electric field is expressed as nominal or true values, i.e. whether the voltage is normalized by the initial or current thickness.
The adopted pre-strain value/s should always be specified, and the environmental temperature and humidity should preferably be mentioned, so as to report the conditions of measurement.

3.8 Electromechanical transduction performance of an elastomer with compliant electrodes and without pre-strain

3.8.1 Basic concepts
There are situations where it is desirable to characterize the actuation strain at zero or minimal pre-strain, such as transducers in which the DE membranes are under minimal tension when not actuated (e.g. because they cannot undergo pre-stretch or because pre-stretching is not applicable). Preventing the film from wrinkling is critically important to allow for accurate measurement of the actuation strain. To this aim, it can be useful to adopt a diaphragm configuration with a nominally low and constant pneumatic pressure, as sketched in Fig. 11, and measure the electrically induced area strain (Ha et al. 2006, Niu et al. 2013).

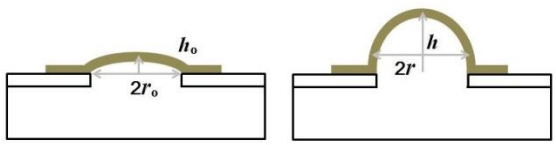

Fig. 11. Diaphragm DEA in the non-activated state (left) and in an electrically activated state (right). The internal pneumatic pressure is kept constant and small.

3.8.2 Measurement method

A DE membrane with active area matching the circular opening of the diaphragm chamber seals the chamber on the top. A small pneumatic pressure (e.g. 300 Pa) is applied underneath causing a minimal pre-strain with a raised height (h_o) that is negligibly small. When actuated, the DE membrane forms a dome shape with a radius r and raised height h. The area strain, S_{Area}, can be calculated by

$$S_{Area} = \frac{(h^2 + r^2) - (h_o^2 + r_0^2)}{h_0^2 + r_0^2} \qquad (27)$$

To measure the radius r and the height h, we recommend the use of contact-less optical techniques, such as processing of images acquired with a digital camera and use of a laser displacement transducer.

The same guidelines presented in section 3.7 for preparation and conditioning of samples, electrical driving and presentation of data apply here as well.

3.9 Electromechanical transduction performance of an elastomer without compliant electrodes

3.9.1 Basic concepts

The electrostatic force needed for DE actuation is commonly generated by coating the elastomer with electrodes and connecting them to a voltage source, so as to charge the soft capacitor. However, in an early experiment in the late 19th century, Wilhelm Conrad Röntgen reported on the electrical deformation of a natural rubber capacitor without compliant electrodes (Röntgen 1880). Röntgen's experiment set the basis for electrode-free DEA operation, enabling later investigations under charge-controlled conditions, inaccessible with compliant-electrode-coated actuators. Indeed, electrode-free actuation has been shown to be a suitable strategy to avoid electromechanical instabilities and to allow for extreme electrically induced deformations limited only by the material's electrical breakdown strength (Keplinger et al. 2010).

Electrode-free actuation is enabled by ions that are generated and induced to rest on the surface of an elastomer film (without electrodes). The ionic charges deposited on the elastomer are immobile, due to the material's low surface conductivity. They thus prescribe "electrically clamped, charge controlled" thermodynamic states. This prevents global electromechanical instabilities, which instead are observed with electrodes and voltage control. Indeed, under voltage control, when the elastomer thins down and expands in area, the electric field increases and so does the attractive force between the electrodes. This creates a positive feedback, causing the elastomer to progressively thin down, finally resulting in electrical breakdown. This global pull-in instability is prevented when the elastomer is operated under charge control, because there is no feedback mechanism which increases the attractive force between the charged surfaces (Keplinger et al. 2010).

Electrode-free operation prevents not only the global instability but also local instabilities. Indeed, with compliant electrodes, charges can easily re-distribute and this may cause local pull-in instabilities. These are prevented with electrode-free operation as charges are immobile and so local breakdowns have no severe consequences for the whole device, because only a small amount of charges is involved (Keplinger et al. 2010).

Therefore, electrode-free operation is useful in material characterization to assess the maximum capabilities of electro-mechanical transduction.

3.9.2 Measurement method

We recommend the use of a circular planar sample, obtained by stretching a DE membrane on a circular frame. Fig. 12 illustrates the setup: charging is performed by spraying charges on the elastomer's surfaces.

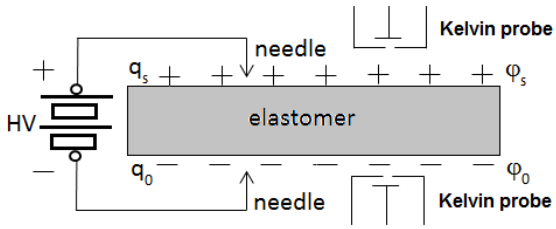

Fig. 12. Illustration of corona charging of an electrode-free DE planar sample.

Any technique known from research on electrets may be employed for charging. In Fig. 12, corona charging is used. Needle electrodes connected to a high voltage source create negatively and positively charged ions. These ions accumulate on the surface of the elastomer, creating spatially dependent charge densities $q_s(x,y)$ and $q_0(x,y)$ on the top and bottom surfaces. The electrostatic forces between these charges cause an electrical deformation of the elastomer. The potential difference (voltage) $V=\varphi_s - \varphi_0$ between the surfaces of the elastomer film must be measured in a non-contact way, as shown in Fig. 12, where two Kelvin probes are used in proximity to the surface.

Actuation performance can be measured with contact-less optical techniques, as described in section 3.7.5.

The same guidelines presented in section 3.7 for preparation and conditioning of samples (except for the electrode material) and presentation of data apply here as well.

4. Device testing

4.1 Static performance of an actuator

The methodology to test the static performance of a DEA is conceptually analogous to the one used to characterise the transduction performance of an elastomer with compliant electrodes. So the reader might refer to that previous section, bearing in mind that the implementation should be adapted to the specific configuration of the device.

4.2 Static performance of a sensor

DE piezo-capacitive sensors make use of the changing capacitance of a loaded DE membrane with compliant electrodes to infer information about mechanical deformation. By way of example, we describe below a method for characterising a uniaxial sensor, for which the relationship between extension and capacitance is approximately linear:

1. Place the sensor in a rig with one end fixed and the other end on a linear stage.
2. Deform the sensor cyclically at different speeds and measure the length independently with a laser, encoder, LVDT or other suitable reference sensor.
3. Measure the capacitance with a suitable interrogation circuit and algorithm (see for instance Gisby et al. 2013) that can compensate for the non-ideal electrode characteristics of the DE sensor.
4. Plot the measured capacitance against extension for a range of different speeds and over a number of cycles in a manner pertinent for the intended application.

The sensor performance can then be defined in terms of the following classical figures of merit:

4.2.1. Drift. Because the output of a DE sensor is directly related to extension, mechanical creep should not cause drift in the signal (this is different when using the sensor to measure force). Drift is thus most likely linked to change in the dielectric constant with temperature (or humidity). Drift can be measured as a change in the baseline or mean capacitance per °C.

4.2.2. Sensitivity. The sensitivity of a DE sensor is the change in capacitance for a given change in extension, i.e. the slope of the capacitance vs extension plot (e.g. F/mm). Sensitivity can be improved by increasing the rest capacitance of the sensor (with layers or by increasing the dielectric constant) or by changing the geometry to make the sensor shorter in the direction of stretch.

4.2.3. Bandwidth. The bandwidth of a DE sensor could be limited by a number of factors, such as latency in the measurement electronics, the size of the sensor, the resistance of the electrodes and connectors, and filters. Limitations to bandwidth can be isolated by introducing delays at different stages in the sensing system and observing the resultant effect.

4.2.4. Noise. Noise in a DE sensor is typically caused by the capacitance measurement circuit. Because sensor capacitances can be small, errors due to parasitic capacitances in the connectors or circuit, thermal noise on components, and minor timing differences in signal acquisition can play a significant role. The position noise can be reduced by increasing the sensitivity of the sensor such that a change in capacitance corresponds to a small change in position.

4.2.5. Hysteresis. When used for deformation sensing, the hysteresis of a DE sensor is typically low because of the dominating effect of geometry on capacitance. When used for force sensing, the mechanical hysteresis can play a role in the accuracy of the sensor and so the choice of the material and the construction of the device should be evaluated according to the specific requirements of the application.

4.2.6. Linearity. A uniaxial extension DE sensor is typically expected to be substantially linear in response. If a pure-shear, equi-biaxial, or a hybrid mode of deformation is used, then the sensor will have a non-linear response.

4.3 Dynamic performance of an actuator

4.3.1 Basic concepts

Any DEA can typically be characterized by two mechanical input/output interfaces, where a force F_m or a displacement x can externally be imposed or electrically generated (note: even a membrane stretched on a frame can be regarded to have two interfaces: the frame and the centre if it is considered as the end effector). So, any lumped-parameter mechanical model of any DEA can be assumed to have two ends. The general model shown in Fig. 13 is considered here to describe the viscoelastic behaviour of a DEA.

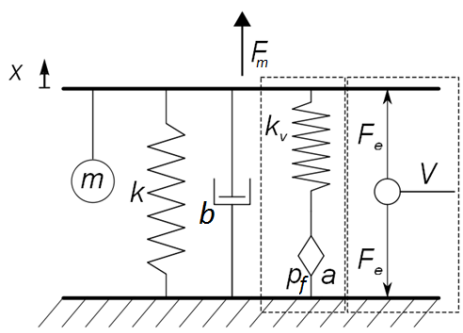

Fig. 13. Example of a dynamic lumped-parameter mechanical model of a DEA.

The model consists of a mass-spring-damper system defined by the parameters m, k and b, respectively, representing a damped oscillator with one degree of freedom and resonant behaviour. The viscoelastic effects typical of many elastomer materials can be taken into account by supplementing the spring and damper with an additional path composed of a spring k_v and a dash-pot in serial configuration, or, more generally, a spring and a fractional element (with parameters p_f and a) describing the viscoelasticity in a wider frequency range (Gaul et al. 1991). The actuation force F_e depends on the input voltage V and is related to the displacement x according to the actuator design. For many DEAs the relationship can be approximated by a quadratic law, owing to the quadratic Maxwell stress (Eq. (4)).
This model can be used to interpret the results of free stroke and blocking force tests, as described below.

4.3.2 Free stroke versus frequency
The dynamic behaviour of DEAs can be characterized in terms of free stroke (displacement) as a function of the excitation frequency. To measure this response, the actuator must be mechanically unloaded and able to move freely, upon driving with a sinusoidal voltage having a constant amplitude (suggested values: 50, 70 and 100% of maximum voltage) and a certain bias (suggested value: equal to the sinusoidal voltage amplitude). The bias voltage is recommended whenever a harmonically oscillating displacement is desired. Indeed, due to the quadratic Maxwell stress law (Eq. (4)), the response of any DEA is always unipolar and therefore a purely sinusoidal voltage lacking of any bias would lead to a unipolar periodic response with doubled frequency.
The actuator has to be clamped at one interface while the displacement is measured at the other one. The measurement should be done with a non-contact system, such as a laser or a capacitive sensor, in order not to influence the measurement mechanically.
A sufficient number of cycles should be allowed to take place in order to reach a steady state. The Fourier coefficients of the input and output signals (the fundamental harmonic) should be calculated and, hence, the amplitude and phase of the transfer function should be determined.
A typical measurement result is shown in Fig. 14, which presents input and output signals at a certain frequency, as well as the amplitude and phase of the transfer function (or frequency response).

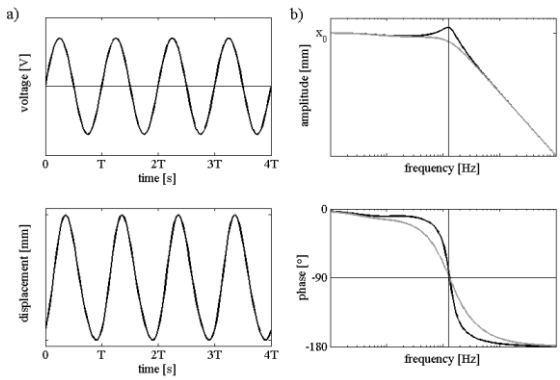

Fig. 14. Example of outcome of the dynamic characterisation of a DEA: a) harmonic voltage signal and corresponding free stroke signal; b) Bode plots of the amplitude and phase of the transfer function (black lines: small damping coefficient; grey lines: large damping coefficient).

The amplitude of the transfer function can show a peak (see the black line in Fig. 14). The frequency at which the highest deformation occurs is defined as the mechanical resonance frequency (or natural frequency).
Above the resonance frequency, the deformation drops down, because of the inertia of the mass and the viscous damping.
If strong viscous damping prevents a distinctive amplitude peak (see the grey line in Fig. 14) the resonance frequency can be determined as the value that causes a phase shift of 90° (Fig. 14).
The resonance frequency can significantly vary according to the masses and mechanical impedances of different boundary conditions.

4.3.3 Blocking force versus frequency
The dynamic behaviour of DEAs can also be characterized in terms of blocking force as a function of the excitation frequency. To this purpose, the actuator is mechanically clamped and a force sensor is included in the test rig. It is necessary to guarantee that, as compared to the actuator, the instrumentation is much stiffer and has no mechanical resonance within the frequency range investigated. Depending on the actuator type and intended use, a given pre-stress can be applied too. A sinusoidal voltage signal is applied with constant bias and amplitude (the same suggestions apply as outlined above). The generated force is measured with a load cell. The Fourier coefficients should be calculated, so as to work out the amplitude and phase of the transfer function.

4.3.4 Mechanical impedance
To determine the passive mechanical behaviour, i.e. to identify the parameters of the viscoelastic model of the device, a mechanical excitation has to be applied. One end is clamped, while a sinusoidal force of amplitude F_m is applied to the other end, and the corresponding displacement x is measured.

Alternatively, a sinusoidal displacement is applied and the corresponding force is measured. Only the first Fourier coefficients of both signals are taken into account. Careful measurement of the relative phasing of both quantities allows for an estimate of the complex mechanical impedance Z_m:

$$Z_m(\omega) = \frac{F_m(\omega)}{v(\omega)} \quad (28)$$

where v is the magnitude of the velocity.

4.3.5 Electrical impedance

DEAs are deformable electrical capacitors (with variable capacitance C), with electrical losses internal to the elastomer (represented by a variable parallel resistance R_p), and ohmic losses introduced by the compliant electrodes and contacts to the power supply (modelled by a variable serial resistance R_S). The resulting electrical equivalent circuit is shown in Fig. 15.

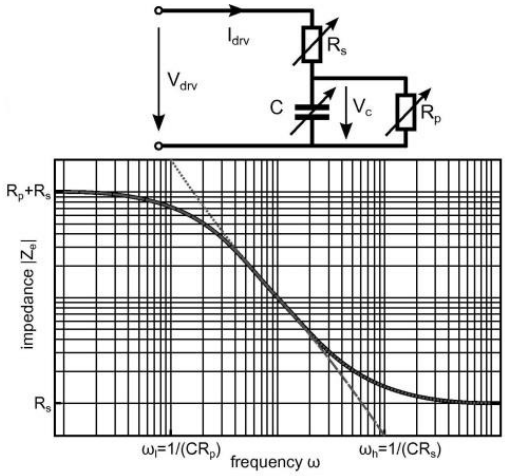

Fig. 15. Simplified electrical equivalent circuit of a DEA and plot of the corresponding electrical impedance versus frequency.

Hence, the electrical impedance Z_e of the DEA is:

$$Z_e = R_s + \frac{1}{\frac{1}{R_p} + j\omega C}\,. \quad (29)$$

and its electrical time constant τ_e is:

$$\tau_e = \frac{R_S R_p C}{R_S + R_p} \quad (30)$$

It is worth noting that if $R_p \gg R_s$, the time constant reduces to $\tau_e \cong R_s C$.

The general frequency dependent behaviour of Z_e is plotted in Fig. 15. We have $Z_e \approx R_p + R_s$ at low frequencies and $Z_e \approx R_s$ at high frequencies. Consistently, the maximum deflection (static mode) can be measured for frequencies $\omega \ll \omega_l = 1/(CR_p)$ because the capacitance will always be fully charged. For frequencies $\omega_l < \omega < \omega_h = 1/(CR_s)$ the voltage across the capacitance is decreasing in inverse proportion to the increasing frequency. For frequencies $\omega \gg \omega_h$ nearly no actuation is possible because the driving voltage drops across R_s as the impedance of the capacitance approaches the lower limit 0.

The electrical impedance can be obtained by using a network analyser. Alternatively, it can be worked out by measuring the current magnitude and phase shift for different frequencies at a fixed voltage magnitude (we recommend at least six frequencies per decade). It is worth noting that the electric shunt used for current measurements has to be designed considering the driving voltage and resulting power.

During impedance measurements, the driving voltage should be significantly smaller (at least 10 times) than the typical actuation voltage, in order to prevent changes of capacitance. To ensure comparability of results, the voltage and internal impedances of the measurement equipment should be reported.

4.3.6 Dynamic limitations of the electrical and mechanical equipment

When dynamic measurements of DEAs are performed, the limitations of the electronic circuitry and the mechanical setup must be taken into account. It is necessary to verify that the frequency range of interest can actually be supplied. In many cases, the range ω_l-ω_h is quite broad; so, it can be challenging to fully explore it without special equipment. Due to the capacitive behaviour of DETs and the fact that any driving source can deliver a maximum current, there exists a maximum frequency up to which the transducer can be fully excited.

4.4 Dynamic performance of a sensor

The methodology to test the dynamic performance of a DES is conceptually analogous to the one used to characterise a DEA. So the reader might refer to the previous section, with an obvious change of the variable of interest.

Nevertheless, an important aspect to be assessed for sensors that are regularly subjected to large tensile strains is the effect that concentration of stress has on the reliability of the sensor/connector interface. Proper cyclic testing, depending on the application requirements, is therefore necessary.

4.5 Efficiency of an actuator

4.5.1 Basic concepts

The electromechanical efficiency is an important and critical figure of merit for any DEA. Depending on the definition used to estimate it, the result can vary according to a diversity of factors, including the operation cycle, the driving frequency, amplitude and bias of the driving voltage, as well as the mechanical impedance of the external load.

Due to the nature of electromechanical coupling in DEAs, all parts of the system (electrical, mechanical and external) are interconnected, such

that the definition of efficiency being considered should always be stated and the operating conditions under which it is measured should always be reported.
So far, a widely shared consensus on how to define general conditions under which the electromechanical efficiency of a DEA should be assessed is not available. The approach recommended here is to drive the actuator with a sinusoidal voltage (having a bias that makes the signal unipolar) and to let it perform work on a load that should be selected according to the actuator configuration and, possibly, its intended use.

4.5.2 Electromechanical efficiency under cyclic operation

In order to estimate the actuator efficiency, the energy losses of the power source should be treated separately from the actuator's inherent electrical energy losses. The former are not considered here, i.e. we assume that the supply circuit fully recovers electrical energy while discharging the actuator. This approach ensures that the electromechanical efficiency is independent of the supply circuit, as long as the supply voltage is controlled, e.g. there is no backlash from the DEA to the power source. In practice, however, the actuator is mostly discharged over a resistance and, hence, the supply circuit does not recover the electrical energy completely, thus decreasing the efficiency of the whole setup (supply circuit plus DEA) but not the actuator electromechanical efficiency itself.
Let us consider the general electrical circuit diagram of an elementary DEA, consisting of a stretch-dependent capacitance with a parallel and serial resistance to account for the actuator's inherent electrical energy losses, as represented in Fig. 15.
The supplied electrical work W_{el} in one cycle (i.e. covering both the charging and discharging phase) under steady-state cyclic operation is:

$$W_{el} = \int_{cycle} V\, I\, dt \qquad (31)$$

where V is the supply voltage applied to the electrical circuit model and I is the current through the circuit. Fig. 16 shows a typical V-Q diagram (for steady-state operation) where Q is the electrical charge supplied to the DEA. The supplied electrical work equals the area encircled by the curve.

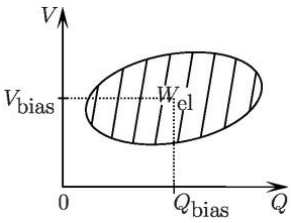

Fig. 16. Example of a steady-state V-Q diagram of a DEA. Here, V_{bias} is the applied bias voltage corresponding to the bias charge Q_{bias} on the capacitor. For an electrically elongating or contractile actuator, the bias voltage results respectively in a positive or negative bias stroke, as long as the load (respectively compressive or tensile) is limited within a certain value. In the final phase of the charging (discharging) process, the voltage decreases (increases) due to the phase shift between voltage and charge caused by the two resistances of the general electrical circuit diagram of the DEA and the conversion of electrical into mechanical work.

The consideration of a steady-state full cycle (an approach commonly used for thermodynamic systems) ensures that no contributions stem from reversible electrical or mechanical energy portions in the actuator.
A fraction of W_{el} is dissipated in the parallel and serial resistances as a work W_{res}, while the remaining part $W_{el-mech}$ is converted into mechanical work by the DE material (owing to the stretch dependence of the capacitance):

$$W_{el-mech} = W_{el} - W_{res} \qquad (32)$$

The mechanical work $W_{el-mech}$ coincides with the effective work performed by the Maxwell stress in a steady-state cycle.
Eq. (32) is the most straightforward way to assess $W_{el-mech}$, if the parallel and serial resistances of the DEA are known. Alternatively, the direct computation of $W_{el-mech}$ via the Maxwell stress is hardly possible for an arbitrary actuator configuration, as quantifying the Maxwell stress is impractical owing to variation of the thickness with strain.
A fraction of $W_{el-mech}$ is dissipated in the dashpots of the viscoelastic model of the DEA as a work W_{visc}, while the remaining part W_{mech_eff} is finally available to perform work on the load:

$$W_{mech\_eff} = W_{el-mech} - W_{visc} \qquad (33)$$

Here, W_{mech_eff} is the effective work performed in one cycle by the DEA, while it is charged and discharged:

$$W_{mech\_eff} = \int_{cycle} F\, \dot{s}\, dt \qquad (34)$$

where F is the force exerted by the actuator (sum of the active and passive forces) on the external load and s is the displacement. Fig. 17 shows a typical F-s diagram (for steady-state operation). The effective work performed in a cycle equals the area encircled by the curve.

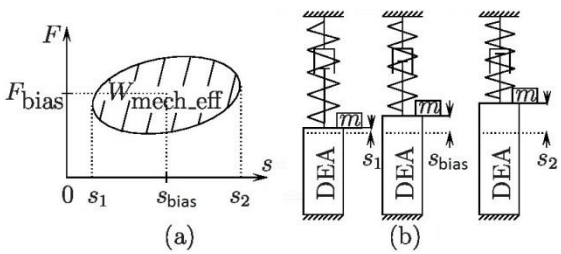

Fig. 17. Example of a steady-state F-s diagram (a) of an actively elongating DEA with a small weight on top of it, such that the bias voltage results in a positive bias stroke (b). In the particular example chosen here, the actuator exerts a positive force on the external load during the whole cycle. The positive bias force might be due to the

DEA, e.g. compressing a spring, besides bearing a small weight. In the final phase of the elongation process, the force decreases due to the phase shift between force and stroke caused by the resistive elements of the external load consuming mechanical work from the DEA. If the external load does not contain any resistive elements, the area encircled by the curve vanishes. If the DEA lifts and sinks a weight infinitesimally slowly, in particular, the F-s curve is a line parallel to the s–axis and its force value equals the gravitational force of the weight.

Fig. 18 shows the flow of work from the power source to the electrical circuit model of the DEA, and then to its viscoelastic model, and finally to the load. The mechanical coupling between DEA and the load and the stretch-dependence of the capacitance are visualized by two backward-oriented arrows.

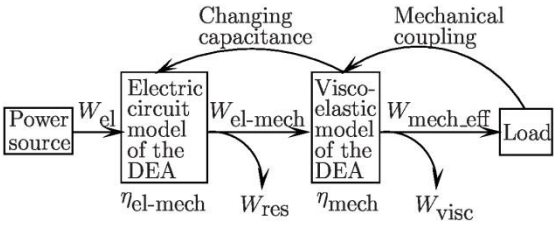

Fig. 18. Work flow for a DEA. The two backward-oriented arrows represent the backlash of the load, first on the viscoelastic model of the DEA and then on its electrical circuit model. This is due to the mechanical coupling between DEA and load, and the dependence of the capacitance on the stretch, respectively.

The actuator's electromechanical efficiency is defined as:

$$\eta = \frac{W_{mech\_eff}}{W_{el}} \tag{35}$$

It can also be expressed as:

$$\eta = \eta_{el-mech}\,\eta_{mech} \tag{36}$$

where $\eta_{el-mech}$ is the electro-mechanical coupling efficiency, defined as the efficiency of the conversion of electrical work into mechanical work:

$$\eta_{el-mech} = \frac{W_{el-mech}}{W_{el}} \tag{37}$$

while η_{mech} is the mechanical coupling efficiency, defined as the efficiency of mechanical work transfer from the DEA to the load:

$$\eta_{mech} = \frac{W_{mech\_eff}}{W_{el-mech}} \tag{38}$$

In some special cases, no work is done on the load in a steady-state cycle ($W_{mech\_eff} = 0$) and, hence, the electromechanical efficiency formally is zero. Notable examples:

i) When there is no load, e.g. the DEA operates in the free stroke mode: in this case, all the electrical work converted into mechanical work during a steady-state cycle is dissipated viscoelastically;

ii) When the load has infinite mechanical impedance, e.g. the DEA operates in the blocking force mode;

iii) When the mechanical impedance of the load is purely imaginary (lossless system), e.g. the DEA stretches and compresses a spring or lifts and sinks a weight. In this case, the work that the DEA performs on the load while elongating is stored reversibly and equals the work that the load performs on the DEA while contracting, or reversely. For example, for an actively contracting actuator that sinks a weight during the charging phase, mechanical work is performed on the DEA and energy is stored reversibly in the device, to be then released to the weight during the discharging phase.

Note that the electromechanical coupling efficiency $\eta_{el-mech}$ defined in this section is different from the square of the electromechanical coupling factor usually defined for piezoelectrics. The electromechanical coupling factor of a DEA is discussed below.

4.5.3 Electromechanical coupling factor

Besides the electromechanical coupling efficiency, the electromechanical coupling factor k is another figure of merit characterizing electromechanical transduction in a DEA. The square of this factor is defined as the ratio between the mechanical energy U_{mech} stored in the DEA and the input electrical energy $U_{el,input}$ at a certain voltage under static free-stroke operation:

$$k^2 = \frac{U_{mech}}{U_{el,input}} \tag{39}$$

The input electrical energy is the sum of the mechanical energy stored in the DEA and the electrical energy stored in the DEA:

$$U_{el,input} = U_{mech} + U_{el} \tag{40}$$

The electrical energy stored in the DEA can be computed from the capacitance of the DEA and the voltage V between the electrodes:

$$U_{el} = \frac{1}{2}CV^2 \tag{41}$$

The mechanical energy can be assessed from the stretch state by an appropriate mechanical model for the DEA. Ideally, the voltage should be applied sufficiently slowly or one should wait sufficiently long before measuring the strain, in order to ensure that dissipative processes do not take place or that they have already taken place. This approach ensures that the electromechanical coupling factor is a figure of merit solely characterizing the DEA, regardless of the operating conditions.

The electromechanical coupling factor measures how much input electrical energy is converted into mechanical energy. Reactive energy portions contribute to the electromechanical coupling factor but not to the electromechanical efficiency.

While the electromechanical coupling factor does not depend on any external load, it does depend on the actuator's geometry and the compliant electrodes. In order to illustrate the dependence on the electrodes, two different DEAs consisting of a single DE sheet sandwiched between two different

types of electrodes are considered below. The description that follows applies to an incompressible (Poisson's ratio $\nu = 0.5$) isotropic material and is limited to small strains, for the sake of simplicity.

The mechanical energy of the DE sheet can easily be inferred from the strain energy density of linear elasticity. If the DE sheet deforms without shear, its mechanical energy is:

$$U_{mech} = \frac{Vol}{3} Y (S_x^2 + S_y^2 + S_z^2) \quad (42)$$

where Vol is the volume of the sheet, Y is the material's Young's modulus, and S_i $(i = x, y, z)$ are the strains in the three Cartesian coordinate directions. Let z denote the thickness direction. In the limit of small strains, the electrical energy stored in the sheet is:

$$U_{el} = \frac{Vol}{2} \varepsilon_0 \varepsilon_r \frac{V^2}{d_0^2} (1 + 2S_z) \quad (43)$$

where d_0 is the thickness of the undeformed DE sheet.

Case 1 - Ideally compliant electrodes:

For ideally compliant electrodes we have $S_x = S_y$ and the incompressibility implies:

$$S_x = S_y = -\frac{S_z}{2} \quad (44)$$

Inserting Eq. (44) in Eq. (42), the mechanical energy stored in the DEA becomes:

$$U_{mech} = \frac{Vol}{2} Y S_z^2 \quad (45)$$

Under free-stroke operation S_z is given by:

$$S_z = -\frac{1}{Y} \varepsilon_0 \varepsilon_r \frac{V^2}{d_0^2} \quad (46)$$

For small strains, $S_z \ll 1$, a good approximation for the electrical energy stored in the DEA is:

$$U_{el} = \frac{Vol}{2} \varepsilon_0 \varepsilon_r \frac{V^2}{d_0^2} \quad (47)$$

The mechanical energy stored in the DEA is:

$$U_{mech} = -S_z U_{el} \quad (48)$$

U_{mech} is much smaller than the electrical energy, and, hence, it can be neglected in Eq. (40) while computing $U_{el,input}$. So, the coupling factor for ideally compliant electrodes is:

$$k^2 = \frac{\varepsilon_0 \varepsilon_r V^2}{Y d_0^2} \quad (49)$$

Case 2 - Electrodes compliant in only one direction:

Let x be the compliant direction and let y be the stiff direction. We have $S_y = 0$ and, due to the incompressibility:

$$S_x = -S_z \quad (50)$$

Therefore, Eq. (42) becomes:

$$U_{mech} = \frac{2}{3} Vol\, Y S_z^2 \quad (51)$$

The free stroke in thickness direction can be derived in the same way as it was done in case 1:

$$S_z = -\frac{3}{4Y} \varepsilon_0 \varepsilon_r \frac{V^2}{d_0^2} \quad (52)$$

For small strains, $S_z \ll 1$, the electrical energy stored in the DEA can again be approximated by Eq. (47) and, doing so, Eq. (48) still holds. Thus, the mechanical energy is much smaller than the electrical energy and can be neglected in Eq. (40). Therefore, the coupling factor for electrodes compliant in only one direction is:

$$k^2 = \frac{3 \varepsilon_0 \varepsilon_r V^2}{4 Y d_0^2} \quad (53)$$

As shown by these examples, the electromechanical coupling factor can be calculated according to the electrical and mechanical properties of the DEA. In case of a linear material, these are the Young's modulus and the dielectric permittivity. In case of a nonlinear material, a similar analysis can be made given a choice of the mechanical constitutive equation (Neo-Hookean, Mooney-Rivlin, Yeoh, etc.) and the result will be expressed in terms of the material parameters of the constitutive relation.

4.5.4 Presentation of data

When reporting electromechanical efficiency, the following parameters should always be specified: i) Frequency, amplitude and bias of the driving voltage; ii) Mechanical impedance of the load; iii) Pre-strain.

4.6 Dynamic performance and efficiency of a generator

4.6.1 Basic concepts

DEG work as soft electrostatic generators capable of harvesting mechanical energy. An initial electrical energy stored into an elastomer film (either pre-stretched or not) is boosted up thanks to mechanically induced deformations (Pelrine et al 2001, Kornbluh et al. 2012). DEGs can operate under various energy conversion cycles according to defined electrical and mechanical specifications, best represented in work conjugate plots. To assess performance, the density of converted energy per cycle and the average output power and efficiency need to be given as functions of numerous parameters. According to the operating area in work conjugate plots, limits of the structure, such as its breakdown voltage, define the maximum allowed energy cycle, as plotted in Fig. 19 using nominal quantities (Koh et al. 2009, Koh et al. 2011).

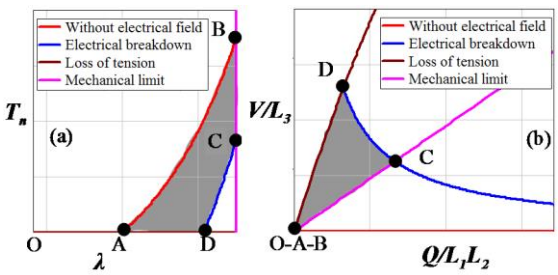

Fig. 19. Allowable operating area for a DEG in pure shear mode with uniform biaxial pre-stretch: (a) Mechanical work conjugate plot; (b) Electric work conjugate plot. T_n is the nominal stress, λ is the stretch ratio, V is the voltage and Q is the electric charge. L_1, L_2 and L_3 are respectively the initial length, width and

thickness of the structure. The area bounded by the points 0-A-B-C-D in a normalised voltage vs normalised charge diagram represents the electrical energy density converted by the DEG without losses (U_{loss}=0), named u_{sca}.

4.6.2 Measurement method

To characterize the dynamic performance of an energy harvester, a deformation of the structure should be imposed at a frequency of interest. An initial pre-stretch λ_p of the structure before the first cycle is recommended. After pre-stretching, the structure should be maintained at electrical rest until relaxation occurs. The generator should generally work under pure shear or biaxial stretch conditions. The complexity of the power circuit might vary, also depending on the application (Jean-Mistral et al. 2008, Eitzen et al. 2012). It should at least not only provide an initial high voltage supply, but should also ensure proper charging and discharging over suitable time lengths, as summarised in Fig. 20 (Foo et al. 2012).

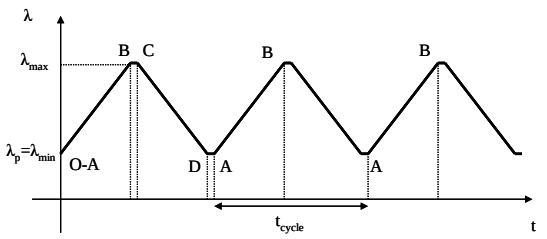

Fig. 20. Recommended time (t)-stretch (λ) curve for a DEG. The maximum and minimum stretches are respectively reached at states B and A defined in the previous figure. The duration of the electrical charging (BC) and discharging (DA) phases must be shorter than the mechanical period t_{cycle}, so as to reduce the influence of electric losses through the dielectric. A constant strain rate $\dot{\lambda}$ should be adopted during the stretching (AB) and relaxation (CD) phases.

At least five cycles are required for the mechanical response to reach a steady state, due to various losses within the DEG structure. Recording of all four external variables (stress, strain, voltage, charge) is preferred (Kaltseis et al. 2011), but at least two of them must be recorded, while the other two may be deduced from modelling. Strains should be measured with a contact-less technique, as structures are highly soft. The voltage should be measured either with an electrostatic voltmeter or with a high-impedance voltage probe (the probe's input resistance should be much larger than the bulk resistance of the dielectric film to prevent discharge during relaxation).

4.6.3 Quantification of performance

To quantify performance, of primary importance is the mechano-electrical conversion efficiency η_{me}:

$$\eta_{me} = \frac{U_e}{U_{mech}} \tag{54}$$

where U_e is the produced electrical energy, namely the final useful energy estimated by taking into account all sorts of losses (electrical and mechanical within the material, and electrical within the power circuit), and U_{mech} is the mechanical energy absorbed by the device over a cycle:

$$U_{mech} = \int F_m ds \tag{55}$$

where F_m is the mechanical force acting on the DEG and s is the displacement.

Fig. 21 describes the overall energy conversion chain. The different types of energy involved are described below.

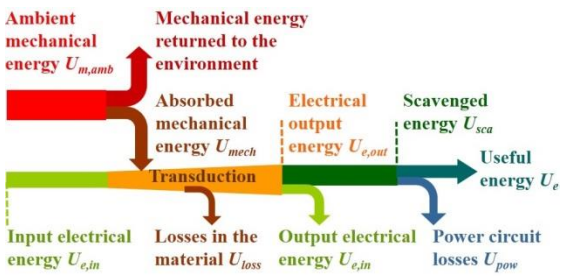

Fig. 21. Energy conversion chain and losses for a DEG.

$U_{m,amb}$ is the ambient mechanical energy. $U_{e,in}$ is the input electrical energy related to the bias voltage and $U_{e,out}$ is the total output electrical energy. U_{sca} is the scavenged electrical energy, defined as follows:

$$U_{sca} = U_{e,out} - U_{e,in} = \int VdQ \tag{56}$$

U_{loss} stands for the energy dissipated by the mechanical viscous losses in a cycle and by the electrical leakage (bulk and surface current). U_{pow} is the energy dissipated by the electrical losses within the power circuit. All the energies represented in Fig. 21 are linked together, as the input mechanical energy U_{mech} must be equal to the output electrical energy U_e plus the losses:

$$U_e = U_{sca} - U_{pow} \tag{57}$$

$$U_{e,out} = U_{mech} + U_{e,in} - U_{loss} \tag{58}$$

$$U_e = U_{mech} - U_{loss} - U_{pow} \tag{59}$$

Regarding the efficiency related to this energy conversion chain, we define the quantities below.

Mechanical absorption efficiency:

$$\eta_{abs} = \frac{U_{mech}}{U_{m,amb}} \tag{60}$$

Device efficiency (taking into account all sorts of material losses, i.e. viscoelastic losses, dielectric losses and ohmic losses at bulk and surface level):

$$\eta_{conv} = \frac{U_{sca}}{U_{mech}} \tag{61}$$

Efficiency of the power management (taking into account the electrical losses in the electrical circuit):

$$\eta_{pow} = \frac{U_e}{U_{sca}} \quad (62)$$

Mechano-electrical conversion efficiency:

$$\eta_{me} = \eta_{conv}\eta_{pow} = \frac{U_{sca}}{U_{mech}}\frac{U_e}{U_{sca}} = \frac{U_e}{U_{mech}} \quad (63)$$

Global efficiency:

$$\eta = \eta_{abs}\eta_{me} = \eta_{abs}\eta_{conv}\eta_{pow} = \frac{U_{mech}}{U_{m,amb}}\frac{U_{sca}}{U_{mech}}\frac{U_e}{U_{sca}} = \frac{U_e}{U_{m,amb}} \quad (64)$$

Several energy densities can be defined and used to compare the performance of different DEGs. We prescribe to name 'density of produced electrical energy per cycle' u_e the volumetric density of electrical energy (expressed in Jcm^{-3}) related to the active volume, i.e. the one composed by the DE membrane and its electrodes:

$$u_e = \frac{U_e}{L_{10}L_{20}L_{30}} \quad (65)$$

where L_{10}, L_{20} and L_{30} are the initial dimensions of the active volume. On the other hand, the 'total density of produced electrical energy per cycle' u_{eTOT} refers to the total volume, i.e. the one which includes not only the active material but also any portion of the dielectric material which is passive, as well as the volume of frames and supports:

$$u_{eTOT} = \frac{U_e}{L_1L_2L_3} \quad (66)$$

where L_1, L_2 and L_3 are the initial dimensions of the entire structure. Following the same principle, the scavenged energy density (u_{sca}, see Fig. 19) and the absorbed energy density can be defined by adopting the same difference for normalisation by either the active volume or the total volume.

To illustrate the performance of a DEG, we recommend that the type of energy cycle (e.g. at constant charge Q), the magnitude of pre-stretch λ_p and the initial bias voltage V_p are first chosen, and then, while maintaining them fixed, one computes how both the efficiency η_{me} and the produced electrical energy density u_e vary versus frequency, i.e. versus the cycle time t_{cycle}, and versus the maximum strain λ_{max} (Fig. 20). The resulting contour plots can be used to describe the frequency-dependent behaviour of the transducer, and to characterise the damping effect and loss factors.

Finally, the generator workspace, generally dedicated to one application, is a trade-off between efficiency and produced electrical energy. We recommend that this workspace is clearly defined and a figure of merit is also defined. Indeed, as the performance of a DEG depends on the bias voltage, the imposed strain, the operating frequency and the energetic cycle, to facilitate performance comparisons between different systems one could use the following figure of merit (FoM):

$$FoM = \frac{u_e}{u_{eMAX}} \quad (67)$$

where u_{eMAX} is the maximum theoretical density of produced electrical energy per cycle, estimated from the electrical diagram representation (Fig. 19). This density refers to the theoretical condition closest to mechanical and electrical breakdown, for the same frequency and energy cycle that produce the energy density u_e.

4.7 Lifetime of a DET

Assessing the lifetime of a DET is very important for applications. Actually, a diversity of performance metrics, such as maximum strain (either achievable from actuation or applicable during stretching in sensor or generator modes), dielectric strength, etc., are scarcely significant without considering lifetime. Indeed, the values for such measurements could vary significantly from a small to a large number of cycles (e.g. millions) (Matysek et al. 2011). However, the current lack of extensive knowledge on the effects of sample preparation and measurement procedures makes it impossible today to define any detailed general protocol (supported by solid physical arguments) to characterise lifetime.

Nevertheless, users seeking for guidelines on how to obtain indicative information might use the suggestions listed below (which are not meant to be prescriptions and might have justified deviations in specific cases). The DET should safely be tested at 80% of its maximum capability (i.e. 80% of maximum electrical strain or stress for a DEA, or 80% of maximum passive deformation for a DES or DEG). It should be solicited with a unipolar alternate stimulus having a fundamental frequency to be selected either according to the application of interest (if known) or equal to 1 Hz (for general-purpose testing). The lifetime could be defined as the time needed to reach a decrease of performance to 50% of the initial value.

5. Future updates

These first set of standards for the DET field are presented with awareness that they are not exhaustive and that they will require future updates. As knowledge in the field will advance and use of these guidelines will spread, deeper insights and further topics will have to be addressed.

Several aspects were deliberately excluded from this first edition, as knowledge and/or consensus in the literature were deemed to be insufficient. The current impossibility of defining guidelines for

several topics is a sign of a young and vital field, whose development is expected to benefit also from this effort towards standardisation.
These standards will be reviewed periodically and we encourage researchers and practitioners to work for future improvements and extensions of the protocols described here.

Acknowledgement

Financial support from COST - European Cooperation in Science and Technology, within the framework of "ESNAM - European Scientific Network for Artificial Muscles" (COST Action MP1003), is gratefully acknowledged.

References

Akbari S., Rosset S., Shea, E. 2013 Improved electromechanical behavior in castable dielectric elastomer actuators, Applied Physics Letters 102 071906.

ASTM D149-09(2013), Standard Test Method for Dielectric Breakdown Voltage and Dielectric Strength of Solid Electrical Insulating Materials at Commercial Power Frequencies, ASTM International, West Conshohocken, PA, 2013, www.astm.org.

Bar-Cohen Y. (2004) Electroactive Polymer (EAP) Actuators as Artificial Muscles: Reality, Potential, and Challenges. SPIE, Bellingham PM136: 1-816.

Biggs J., Danielmeier K., Hitzbleck J., Krause J., Kridl T., Nowak S., Orselli E., Quan X., Schapeler D., Sutherland W., Wagner J., Electroactive Polymers: Developments of and Perspectives for Dielectric Elastomers, Angew. Chem. Int. Ed. 52, 9409-9421, 2013.

Boyce MC and Arruda EM 2000 Constitutive Models of Rubber Elasticity: A Review Rubber Chemistry and Technology 73 504-523.

Brochu P and Pei Q. (2010) Advances in dielectric elastomers for actuators and artificial muscles. Macromol Rapid Commun 31: 10-36.

Carpi F and Smela E. (2009) Biomedical Applications of Electroactive Polymer Actuators. Wiley, Chichester, UK.

Carpi F, De Rossi D, Kornbluh R, Pelrine R, Sommer-Larsen P. (2008) Dielectric Elastomers as Electromechanical Transducers: Fundamentals, materials, devices, models and applications of an emerging electroactive polymer technology. Elsevier, Oxford, UK.

Carpi F., Bauer S. De Rossi D. Stretching dielectric elastomer performance, Science 330, 1759, 2010.

Carpi F, De Rossi D, Improvement of electromechanical actuating performances of a silicone dielectric elastomer by dispersion of titanium dioxide powder, IEEE Transactions on Dielectrics and Electrical Insulation, Vol. 12(4), pp. 835-843, 2005.

Carpi F, Gei M. Predictive stress-stretch models of elastomers up to the characteristic flex. Smart Materials and Structures 22, 104011, 2013.

Carpi F., Chiarelli P., Mazzoldi A., De Rossi D. Electromechanical characterisation of dielectric elastomer planar actuators: comparative evaluation of different electrode materials and different counterloads", Sensors And Actuators A - Physical, 107, 85-95, 2003.

Choi H. R., Jung K., Chuc N. H., Jung M., Koo I., Koo J., Lee J., Lee J., Nam J., Cho M., Lee Y., 2005 Effects of Prestrain on Behavior of Dielectric Elastomer Actuator, Proc. SPIE **5759** 283.

Danfoss PolyPower A/S white paper, PolyPower® DEAP material. Available online (May 2014) at http://www.polypower.com/NR/rdonlyres/0512EB3D-6232-46DD-9F86-43B389D9059E/0/094F5001WhitepaperPolyPowerDEAPmaterial.pdf

Eitzen L., Graf C. and Maas J. 2012 Bidirectional Power Electronics for Driving Dielectric Elastomer Transducers *Proc. SPIE* 8340, 834018.

Foo C. C. , Koh S. J. A. , Keplinger C., Kaltseis R., Bauer S. and Suo Z. Performance of dissipative dielectric elastomer generators J. Appl. Phys. 111 094107, 2012.

Gatti Davide, Haus Henry, Matysek Marc, Frohnapfe Bettina, Tropea Cameron and Schlaak Helmut F., The dielectric breakdown limit of silicone dielectric elastomer actuators, Applied Physics Letters 104, 052905 (2014).

Gaul L., Klein P., Kemple S., Damping description involving fractional operators, Mechanical Systems and Signal Processing, Volume 5, Issue 2, 1991, Pages 81-88.

Gisby T A, O'Brien B M, Anderson I A 2013 Self sensing feedback for dielectric elastomer actuators *Applied Physics Letters* 102 193703-4.

Ha S.M., W. Yuan, Pei Q., Pelrine R. and Stanford S., Interpenetrating Polymer Networks for High-Performance Electroelastomer Artificial Muscles, Advanced Materials 18, 887–891 (2006).

Huang Jiangshui, Li Tiefeng, Foo Choon Chiang, Zhu Jian, Clarke David R., and Suo Zhigang. (2012b). Giant, voltage-actuated deformation of a dielectric elastomer under dead load, Applied Physics Letters 100(4): 041911.

Huang Jiangshui, Shian Samuel, Diebold Roger M., Suo Zhigang, and Clarke David R., The thickness and stretch dependence of the electrical breakdown strength of an acrylic dielectric elastomer, Applied Physics Letters 101, 122905 (2012a).

Jean-Mistral C., Basrour S. and Chaillout J.-J. Dielectric polymer: scavenging energy from human motion Proc. SPIE 6927 692716, 2008.

Kaltseis R., Keplinger C., Baumgartner R., Kaltenbrunner M., Li T., Maechler P., Schwoediauer R., Suo, Z. and Bauer S. Method for measuring energy generation and efficiency of dielectric elastomer generators, Appl. Phys. Lett. 99, 162904, 2011.

Keplinger C. Kaltenbrunner M., Arnold N., and Bauer S. Capacitive extensometry for transient strain analysis of dielectric elastomer actuators, Appl. Phys. Lett. 92, 192903, 2008.

Keplinger C., Kaltenbrunner M., Arnold N., and Bauer S. Röntgen's electrode-free elastomer actuators without electromechanical pull-in instability PNAS 107 4505-4510. 2010.

Kofod, G., Sommer-Larsen, P., Kronbluh, R. and Pelrine, R. (2003) Actuation response of polyacrylate dielectric elastomers. Journal of Intelligent Material Systems and Structures, 14, 787.

Kofod G., Sommer-Larsen P. 2005 Silicone dielectric elastomer actuators: Finite-elasticity model of actuation, Sensors and Actuators A: Physical 122 273–83.

Koh S.J.A., Keplinger C., Li T., Bauer S. and Suo Z. Dielectric elastomer generators: how much energy can be converted. IEEE/ASME Transactions on Mechatronics 16, 33-41, 2011.

Koh, S.; Li, T.; Zhou, J.; Zhao, X.; Hong, W.; Zhu, J. & Suo, Z. Mechanisms of large actuation strain in dielectric elastomers, Journal of Polymer Science, Part B: Polymer Physics, 49, 504-515, 2011.

Koh S.J.A., Zhao X. and Suo Z. Maximal energy that can be converted by a dielectric elastomer generator Applied Physics letters 94 262902, 2009.

Kollosche, M. and Kofod, G. 2010. Electrical failure in blends of chemically identical, soft thermoplastic elastomers with different elastic stiffness. Applied Physics Letters, 96, 071904.

Kollosche Matthias, Zhu Jian, Suo Zhigang, and Kofod Guggi (2012). Complex interplay of nonlinear processes in dielectric elastomers, Physical Review E, 85, 051801.

Kornbluh R., Pelrine R., Prahlad H., Foy A.W., McCoy B., Kim S., Eckerle J. and Low T. Dielectric elastomers: Stretching the capabilities of energy harvesting, MRS Bull. 37 (3), 246-253, 2012.

Matysek M., Lotz P., Schlaak H. F., Lifetime investigation of dielectric elastomer stack actuators, IEEE Transactions on Dielectrics and Electrical Insulation, 2011, 18(1):89-96.

Moreno C., Hernández S., Santana J.J., González-Guzmán J., Suoto R.M., González S., Characterization of Water Uptake by Organic Coatings Used for the Corrosion Protection of Steel as Determined from Capacitance Measurements, Int. J. Electrochem. Sci., 7, 8444 – 8457, 2012.

Mullins L 1969 Softening of rubber by deformation. *Rubber Chemistry and Technology* 42, 339-362.

Niu Xiaofan, Stoyanov Hristiyan, Hu Wei, Leo Ruby, Brochu Paul and Pei Qibing, Synthesizing a new dielectric elastomer exhibiting large actuation strain and suppressed electromechanical instability without prestretching, J. Polymer Science, Part B: Polymer Physics, 51, 197–206 (2013).

Oertel G 1993 *Polyurethane Handbook*, 2nd edn, Hanser Verlag, München.

Ogden R W 1997 *Non-linear Elastic Deformations*, Dover, New York.

Ogden, R.W., Roxburgh, D.G. (1999) A pseudo-elastic model for the Mullins effect in filled rubber. Proc. Roy. Soc. Lond. A455, 2861-2877.

Pelrine R., Kornbluh R., Eckerle J., Jeuck P., Oh S., Pei Q. and Stanford S. Dielectric elastomers: generators mode fundamentals and its applications, Proc. SPIE 4329, 148-156, 2001.

Pelrine R., Kornbluh R., Pei Q. and Joseph J. 2000 High-speed electrically actuated elastomers with strain greater than 100% Science 287 836.

Reuge, N.; Schmidt, F.; Le Maoult, Y.; M., R. & Abbe, F. Elastomer biaxial characterization using bubble inflation technique. I: Experimental investigations Polymer Engineering and Science, 2001, 41, 522-531.

Rivlin R S and Saunders D W 1951 Large elastic deformations of isotropic materials. VII. Experiments on the deformation of rubber *Phil. Trans. R. Soc. Lond. A* **243** 251-288.

Rosset S, Maffli L, Houis S, Shea H. 2014 An instrument to obtain the correct biaxial hyperelastic parameters of silicones for accurate DEA modelling. Proc. SPIE 9056, 90560M.

Rosset, S.; Shea, H. (2013). Flexible and stretchable electrodes for dielectric elastomer actuators. Appl Phys. A. 110 281–307.

Rosset Samuel, O'Brien Benjamin, Gisby Todd, Xu, Daniel, Shea Herbert and Anderson Iain (2013), Self-sensing dielectric elastomer actuators in closed loop operation, Smart Mater. Struct. 22, 104018-1 - 104018-10.

Röntgen W. C. 1880 Ueber die durch Electricität bewirkten Form- und Volumenänderungen von dielectrischen Körpern Ann. Phys. Chem. 11 771-786.

Suo Z. Theory of dielectric elastomers. Acta Mechanica Solida Sinica, 2010, 23, 549-578.

Suratkar A. 2009 Absolute Distance (Thickness) Metrology Using Wavelength Scanning Interferometry, *PhD Dissertation*, University of North Carolina, p. 9.

Treloar LRG (1944) Stress–strain data for vulcanized rubber under various types of deformation. Trans. Faraday Soc. 40: 59–70.

Troels Andreas, Alexander Kogler, Richard Baumgartner, Rainer Kaltseis, Christoph Keplinger, Reinhard Schwodiauer, Ingrid Graz and Siegfried Bauer, Stretch dependence of the electrical breakdown strength and dielectric constant of dielectric elastomers, Smart Mater. Struct. 22 (2013) 104012.

Weibull W 1951 A statistical distribution function of wide applicability *J. Appl. Mech*. 18, 293-297.

Wissler Michael, Mazza Edoardo, Electromechanical coupling in dielectric elastomer actuators, Sensors and Actuators A 138 (2007) 384–393.